



HAL
open science

Annelid polychaetes experience metabolic acceleration as other Lophotrochozoans: inferences on the life cycle of *Arenicola marina* with a Dynamic Energy Budget model

Lola de Cubber, Sébastien Lefebvre, Théo Lancelot, Lionel Denis, Sylvie Marylène Gaudron

► To cite this version:

Lola de Cubber, Sébastien Lefebvre, Théo Lancelot, Lionel Denis, Sylvie Marylène Gaudron. Annelid polychaetes experience metabolic acceleration as other Lophotrochozoans: inferences on the life cycle of *Arenicola marina* with a Dynamic Energy Budget model. *Ecological Modelling*, 2019, 411, pp.108773. 10.1016/j.ecolmodel.2019.108773 . hal-02408975

HAL Id: hal-02408975

<https://hal.sorbonne-universite.fr/hal-02408975>

Submitted on 13 Dec 2019

HAL is a multi-disciplinary open access archive for the deposit and dissemination of scientific research documents, whether they are published or not. The documents may come from teaching and research institutions in France or abroad, or from public or private research centers.

L'archive ouverte pluridisciplinaire **HAL**, est destinée au dépôt et à la diffusion de documents scientifiques de niveau recherche, publiés ou non, émanant des établissements d'enseignement et de recherche français ou étrangers, des laboratoires publics ou privés.

1 Annelid polychaetes experience metabolic acceleration as other
2 Lophotrochozoans: inferences on the life cycle of *Arenicola*
3 *marina* with a Dynamic Energy Budget model

4 Lola De Cubber^{a,*}, Sébastien Lefebvre^a, Théo Lancelot^a, Lionel Denis^a, Sylvie Marylène
5 Gaudron^{a,b}

6 ^aUniv. Lille, Univ. Littoral Côte d'Opale, CNRS, UMR 8187 Laboratoire d'Océanologie et de Géosciences, 62930
7 Wimereux, France

8 ^bSorbonne Univ., UFR 918 & UFR 927, 75005 Paris, France

9 **Abstract**

10 *Arenicola marina* is a polychaete (Lophotrochozoan) displaying a complex benthic-pelagic life
11 cycle with two larval dispersal phases, only partially described up to now. A Dynamic Energy
12 Budget (DEB) model was applied to the species in order to reconstruct its life cycle and growth
13 under *in situ* environmental conditions. Two types of DEB models are usually applied to other
14 Lophotrochozoans displaying similar life cycles: the standard (std-) model, applied to polychaetes
15 (5 entries among the 1524 of the Add-my-Pet database on the 18/10/2018), and the abj-model,
16 which includes an acceleration of metabolism between birth and metamorphosis, and which has
17 been applied to most molluscs (77 abj- entries out of the 80 mollusc entries) enabling better fit
18 predictions for the early life stages. The parameter estimation was performed with both models to
19 assess the suitability of an abj-model for *A. marina*. The zero-variate dataset consisted of length
20 and age data at different life cycle stages, the lifespan, the maximum observed length, and the wet
21 weight of an egg. The uni-variate dataset consisted of two growth experiments from the literature
22 at two food levels and several temperatures, laboratory data of oxygen consumption at several
23 temperatures, and fecundity for different lengths. The predictions of the abj-model fitted better to
24 the data (SMSE = 0.29). The acceleration coefficient was *ca* 11, which is similar to mollusc values.
25 The field growth curves and the scaled functional responses (as a proxy of food levels) were suitably
26 reconstructed with the new parameter set. The reconstruction of the early life-stages chronology
27 according to *in situ* environmental conditions of a temperate marine ecosystem indicated a first
28 dispersal phase of 5 days followed by a 7 months temporary settlement before a second dispersal
29 phase in spring, at the end of metamorphosis. We emphasize the need for using abj-models for
30 polychaetes in future studies.

31 **Key words**

32 Bioenergetics, lugworm, growth, oxygen consumption, life-history traits, dispersal

*Corresponding author: lola.decubber@gmail.com

33 Introduction

34 *Arenicola marina* (Linnaeus, 1758) is a marine polychaete (Lophotrochozoan, Annelida) inhab-
35 iting most intertidal soft sediments from the Arctic to the Mediterranean. The species is intensively
36 dug for bait by recreational fishermen (Blake, 1979; De Cubber et al., 2018; Watson et al., 2017)
37 and the comparison between harvest efforts and observed populations abundance has evidenced
38 the need for some regulation of this activity in some places (De Cubber et al., 2018). In aquacul-
39 ture, *A. marina* is also reared for bait (Olive et al., 2006), and more recently, for its particular
40 haemoglobin that might represent a valuable blood substitute for humans in the future (Rousselot
41 et al., 2006) and which is already used for organs conservation before transplantation. However,
42 its complex benthic-pelagic life cycle with two dispersal phases before recruitment has made the
43 description of the early life stages and their chronology complicated, and still little is known about
44 the development of *A. marina* between the trochophore larva stage and the benthic recruitment
45 (Farke and Berghuis, 1979a, b; Newell, 1948; Reise, 1985). Moreover, the literature regarding *A.*
46 *marina*'s life cycle and growth is quite ancient (mostly from 1979) and since 1990, it has been found
47 that two cryptic species actually exist and might live in sympatry: *A. marina* and *A. defodiens*.
48 Therefore ancient life-history description has to be used with caution (Cadman and Nelson-Smith,
49 1990).

50 The 'Dynamic Energy Budget' (DEB) theory quantifies the energy allocation to growth and
51 reproduction of an individual during its life cycle according to environmental conditions such as
52 temperature and food availability (Kooijman, 2010) even in species with complex and numerous
53 life-stages (Llandres et al., 2015). Twelve primary parameters are sufficient for the implementation
54 of a standard (std-) DEB model. However, among the assumptions implied in std-DEB models,
55 some, like isomorphism during growth, the fact that growth always follows a typical Von Bertalanffy
56 growth curve, or the presence of three life stages (embryo, juvenile and adult) are not found in every
57 species. Therefore, extensions of the std-model (implying the use of more parameters) were created
58 (Kooijman, 2014) accounting for deviations from typical development implied by the std-model,
59 like foetal development, acceleration of metabolism, or extra life stages.

60 As of October 2018, Add-my-Pet (AmP) database estimated DEB parameters for 1524 animal
61 species (Marques et al., 2018). Among these entries, only 11 were annelid species, 4 of them being
62 polychaetes species for which std-models were applied. The closest phylum with a large amount
63 of data is the molluscs' phylum (over 80 entries), also presenting a larval stage. Indeed, annelids
64 and molluscs belong to the Lophotrochozoan clade and both, after the embryogenesis, lead to a
65 trochophore larval stage. Mostly abj-DEB models have been applied only for the mollusc phylum,
66 which are an extension of std-models considering an acceleration of metabolism between birth (first
67 feeding) and metamorphosis (end of the change of shape) and are applied to most species with a
68 larval phase (Kooijman, 2014). Although polychaete species often present a larval phase during
69 their life cycle, until now, abj-models were not applied to this taxa.

70 A std- entry for *A. marina* is present in the AmP database and enables predictions of the
71 growth and reproduction of the species. However, more than half of the dataset used for the
72 parameter estimation consists of unpublished data (time since birth at puberty and maximum
73 reproduction rate taken from Marlin: <https://www.marlin.ac.uk/> and lifespan and ultimate total
74 length taken from Wikipedia: <https://www.wikipedia.org/>), guessed data (wet weight at birth and
75 puberty, ultimate wet weight), or data related to other species (age at birth from *A. cristata* and
76 *A. brasiliensis*) (AmP entry: Bas Kooijman. 2015. AmP *Arenicola marina*, version 12/07/2015).
77 We therefore completed the data set with literature, experimental and field data, and implemented
78 a new parameter estimation for the species using both a std- and an abj-DEB models.

79 The objectives were:

- 80 (1) to calibrate a DEB model for *A. marina* based on a reliable and complete dataset and
81 adapted to its life cycle features (and therefore to compare the relevance of the use a std- or
82 an abj-DEB model for this species)
- 83 (2) to make predictions about the chronology of the early life stages of *A. marina* and the growth
84 potential according to the environmental conditions
- 85 (3) to compare the parameters of the DEB models implemented for *A. marina* with the other
86 Lophotrochozoan species' parameters and discuss the advantages of the use of an abj-model
87 for this species.

88 1. Material and Methods

89 1.1. The DEB theory and its implementation for *Arenicola marina*

90 1.1.1. The model

91 The DEB theory describes the energy flows within an organism between three compartments
92 (state variables) : the reserve (E), the structure (V), and the maturity (E_H) or the reproduction
93 buffer (offsprings) (E_R) according to its life stage in order to describe its energy allocation to
94 growth and reproduction for a given food level and at a reference temperature T_{ref} (Fig. 1). The
95 three differential equations linked to the state variables are obtained from the expression of the
96 different fluxes (Table 1)(Kooijman, 2010; Van der Meer, 2006).

97 Temperature corrections are made to the rates considered by the model in the equation of
98 fluxes (e.g. the surface-area specific maximum assimilation rate, $\{\dot{p}_{Am}\}$ ($\text{J}\cdot\text{cm}^{-2}\cdot\text{d}^{-1}$), the energy
99 conductance, \dot{v} ($\text{cm}\cdot\text{d}^{-1}$), the specific volume-linked somatic maintenance rate, $[\dot{p}_M]$ ($\text{J}\cdot\text{cm}^{-3}\cdot\text{d}^{-1}$),
100 and the maturity maintenance rate coefficient, \dot{k}_J (d^{-1}), see Tables 1 and 4). Indeed, when the
101 temperature T (K) is different from the reference temperature T_{ref} (taken to be 293.15 K) these
102 rates are multiplied by the correction given in Equation (1), where T_A is the Arrhenius temperature
103 (K), \dot{k}_1 the rate of interest at T_{ref} and \dot{k} the rate of interest at T .

$$\dot{k}(T) = \dot{k}_1 \cdot \exp\left(\frac{T_A}{T_{ref}} - \frac{T_A}{T}\right) \quad (1)$$

104 The links between observable metrics (physical length and wet weight) and the DEB model
 105 quantities are made with the shape coefficient δ (varying between $\delta = \delta_{Me}$ for embryos and $\delta = \delta_M$
 106 after metamorphosis), the density of wet structure d_V ($g.cm^{-3}$), of wet reserve d_E ($g.cm^{-3}$) and of
 107 dry reserve d_{Ed} ($g.cm^{-3}$), the specific chemical potential of reserve μ_{Ed} ($J.Cmol^{-1}$ of reserve), and
 108 the molar weight of reserve w_{Ed} ($g.Cmol^{-1}$) (Table 1). Here, we assumed that $d_V = d_E = 1 g.cm^{-3}$,
 109 $d_{Ed} = 0.16 g.cm^{-3}$, $\mu_{Ed} = 550000 J.Cmol^{-1}$ and that $w_{Ed} = 23.9 g.Cmol^{-1}$.

110 1.1.2. Adaptation to *Arenicola marina*'s life cycle

111 The spawning event of *Arenicola marina* happens in late summer or early autumn (De Cubber
 112 et al., 2018; Watson et al., 2000). After the external fertilization, the embryo develops in the female
 113 gallery up to the post-embryonic stage, the trochophore larva, which is able to move vertically in
 114 the water column (Fig. 2, Farke and Berghuis, 1979a, b). At this time, the shape is changing
 115 from ovoidal (oocytes, with a shape coefficient $\delta = \delta_{Me}$) to cylindrical when the trochophore larva
 116 gradually acquires new setiger becoming a metatrochophore larva (of shape coefficient $\delta < \delta_{Me}$).
 117 The metatrochophore larva is released in the water column when it reaches 3 setigers and is
 118 transported by currents during several days. In lugworms, embryos and larvae are lecithotrophic,
 119 living on maternal reserve and therefore supposed not to be able to feed (the maturity threshold
 120 E_H did not yet reach its value for birth: $E_H < E_H^b$, where birth is the time when individuals start
 121 to feed). Therefore, there is no feeding or assimilation flux during the embryo and larval stage and
 122 $dE/dt = -\dot{p}_C$ (Table 1). Moreover, these young stages do not have enough complexity yet to be
 123 able to produce gametes and the reproduction flux goes to maturity (Table 1), which represents in
 124 this case the acquisition of complexity of the individual (Fig. 1).

125 The metatrochophore larva settles and begins eating as post-larva, when the gut appears func-
 126 tional ($E_H = E_H^b$), either on mussel beds, macroalgae or sheltered soft sediment bottoms (Fig.
 127 2). At this point, it lives inside a mucus tube stuck to the bottom and feeds on the particles
 128 deposited on the tube and around it, as well as on suspended particles (Farke and Berghuis, 1979a,
 129 b; Newell, 1949; Reise, 1985; Reise et al., 2001). During this temporary settlement period, the
 130 post-larva continues to gradually acquire new setigers up to the 19 final setigers found in adults
 131 (the shape coefficient δ keeps on decreasing until it reaches the shape coefficient value of the adults
 132 δ_M), developing a proboscis in the way of the adults (Farke and Berghuis, 1979a, b; Newell, 1949).
 133 These morphological changes are assimilated to metamorphosis (up to when the maturity threshold
 134 E_H reaches its value at metamorphosis: $E_H = E_H^j$). During this period, a metabolic acceleration
 135 (Kooijman, 2014) was considered, which is supposed to happen in most species that have a lar-
 136 val phase, frequently coinciding with morphological metamorphosis (Marques et al., 2018), and
 137 resulting in an exponential growth of the organism between the first feeding and the end of meta-
 138 morphosis. From birth ($E_H = E_H^b$), feeding and assimilation are not null anymore, but individuals
 139 are not able yet to produce gametes ($\dot{p}_R = 0$).

140 When metamorphosis ends, a second dispersal phase of unknown period occurs in the water

141 column and the newly juvenile lugworm settles on intertidal areas colonized by adults' lugworms,
142 where it changes its mode of nutrition, becoming psammivorous like the adults (Beukema and De
143 Vlas, 1979)(Fig. 2). The shape coefficient value stops changing, the growth starts to be isomorphic
144 and follows the Von Bertalanffy growth curve for a constant scaled functional response (Kooijman,
145 2010), but it is not yet able to reproduce like the adults (since the maturity threshold E_H did not
146 reach its value at puberty yet: $E_H < E_H^p$).

147 Finally, the adults acquire the ability to reproduce (which is when $E_H > E_H^p$) and the energy
148 flow formerly allocated to maturity is transferred to a reproduction buffer (offsprings) that empties,
149 in the case of *Arenicola marina*, once a year in early autumn, during the spawning event.

150 1.2. Compilation of data for *Arenicola marina* and parameter estimation

151 1.2.1. Zero-variate and uni-variate data from the literature

152 *Zero-variate data from the literature.* An important part of the zero-variate dataset found in the
153 literature was composed of data taken from a larval culture performed by Farke and Berghuis
154 (1979) before 1990, when the two species *Arenicola marina* and *A. defodiens* were not yet delimited
155 (Cadman and Nelson-Smith, 1993): the lengths at trochophore larva, at birth (first feeding) and at
156 metamorphosis with their associated ages (Table 5). Although the lengths data seem quite accurate
157 (plates and pictures), the chronology description made by the authors remains vague. The precise
158 time line had thus to be estimated from sometimes quite confused date references and we gave a
159 weight of 0.5 to this data in the parameter estimation procedure. In the larval culture performed
160 by Farke and Berghuis (1979), the temperature varied from 8 to 16 °C, so a mean temperature of
161 12 °C was used for the data taken from this experiment.

162 The second part of the zero-variate dataset from the literature was collected after 1990. First,
163 the age for the occurrence of the trochophore larva at 10 °C was communicated by S. Gaudron
164 from unpublished *in vitro* fertilization experiments. The maximum observed trunk length (good
165 biometric estimate, see De Cubber et al., 2018) was observed by S. Gaudron on a specimen kept
166 in the Animal Biology Collection of the Sorbonne University (France). Finally, the age and length
167 at puberty, the oocyte diameter and the lifespan were previously acquired by the authors at the
168 same study site (De Cubber et al., 2018). The temperature used for this data was the mean
169 temperature of the seawater over the year 2017 (13 °C, SOMLIT data: [http://somlit-db.epoc.u-](http://somlit-db.epoc.u-bordeaux1.fr/)
170 [bordeaux1.fr/](http://somlit-db.epoc.u-bordeaux1.fr/), bottom coastal sampling point at Wimereux). The age and the trunk length at
171 puberty corresponded to a first mature adult of 2.5 cm and 1.5 years old. All the age data estimated
172 from length analysis were given a weight of 0.5 in the parameter estimation procedure considering
173 their potentially low accuracy. For all zero-variate data the f value was set to 1, considering that
174 only the "best individuals" were used.

175 *Uni-variate data from the literature.* The uni-variate dataset retrieved from the literature consisted
176 in the datasets of two growth experiments:

- 177 - One growth experiment in which trunk length was measured at four different temperatures
178 (5, 10, 15 and 20 °C) under two different food conditions (fed and unfed) taken from De
179 Wilde and Berghuis (1979) (8 treatments). The corresponding f values were set at $f_{fed} = 0.8$
180 and $f_{unfed} = 0.1$ in view of growth comparisons made by the authors in the same study.
- 181 - One growth experiment in which wet weight was measured at one temperature varying be-
182 tween 16 and 20°C under two different conditions (fed and unfed) taken from Olive et al.
183 (2006) (2 treatments). Temperature was set at 19.5°C and the f values were left free for both
184 conditions.

185 For these two growth experiments, the temperature and feeding conditions met before the start
186 of the experiment were not known so we had to assume the levels of reserve and structure at the
187 beginning of the experiment. Therefore, predictions of growth could only be made considering a
188 physical trunk length $TL_w(0)$ at the beginning of the experiment and a physical wet weight $W_w(0)$
189 at the beginning of the experiment equalling to the one of the experiment.

190 1.2.2. Laboratory experiments and field data

191 Additional reproductive data (reproduction rate as a function of trunk length and wet weight
192 of an egg), growth data (trunk length over time) and oxygen consumption data (oxygen consump-
193 tion as a function of wet weight) were acquired by the authors in the laboratory and from field
194 observations between 2016 and 2018 in order to complete the dataset collected from the literature.

195 *Study area and sampling strategy.* Lugworms were collected at Wimereux (N 50°46'14" and E
196 01°36'38"), Le Touquet (N 50°31'07" and E 01°35'42") and Fort Mahon (N 50°20'31" and E
197 01°34'11"), located in the Eastern English Channel (Hauts-de-France, France)(Table 2). More
198 details on the sites are given in De Cubber et al. (2018). For the oxygen consumption experiment
199 (Exp. A), the lugworms were collected at Wimereux from the high mediolittoral to the high in-
200 fralittoral part of the foreshore (Fig. 2), in order to collect all the different age groups and sizes
201 (De Cubber et al., 2018), on the sandy beach part, using a shovel. Collection happened three times
202 between May and July 2018 in order to follow the summer increase of the seawater temperature
203 of the English Channel (Table 2). For the reproductive data (Exp. B), ripe females of *A. marina*
204 were collected at Wimereux, Le Touquet and Fort Mahon using a shovel or a bait pump (Decathlon
205 ltd.) during the spawning period of each year (Table 2). For the growth experiment (Exp. C),
206 young individuals of *A. marina* were collected at Wimereux on the high mediolittoral part of the
207 foreshore with a shovel (De Cubber et al., 2018) at the end of May 2018 (Table 2, see more details
208 in De Cubber et al., 2018).

209 *Laboratory measurements.* After each sampling, all lugworms were put in separate containers filled
210 with seawater. Individuals of *Arenicola marina* were maintained in the laboratory during 24 h at
211 the temperature of the English Channel at Wimereux at the time of their collection (12, 15 and

212 20.5 °C) for the oxygen consumption experiment (Exp. A), and at 15 °C otherwise (Exp. B and
213 C), in a cold room, to allow gut to be devoided of their content prior to observations (Watson et
214 al., 2000). Biometric measurements consisted in total length, trunk length (more reliable, see De
215 Cubber et al., 2018 and De Wilde and Berghuis, 1979), and in wet weight measurements.

216 *Experiment A: Oxygen consumption.* The oxygen consumption rates of lugworms were recorded
217 as a proxy of metabolic activity (Galasso et al., 2018). Metabolic rates can vary between two
218 fundamental physiological rates, one minimal maintenance metabolic rate (the standard metabolic
219 rate) and one maximum aerobic metabolic rate (the active metabolic rate) (Galasso et al., 2018;
220 Norin and Malte, 2011). In order to recreate these two situations of activity in the laboratory, and
221 avoid any over- or underestimation of the metabolic rate, the oxygen consumption of lugworms was
222 measured under two different conditions in which their metabolic activity was supposed close to
223 the standard metabolic rate on one hand, and close to the active metabolic rate on the other hand.
224 In the condition in which lugworms were supposed to experience a standard metabolic rate, around
225 30 of the collected individuals were transferred into Eppendorfs or Falcon centrifuge tubes (5 ml
226 or 50 ml according to the size of the worms) half-filled with sand from Wimereux burnt at 550°C
227 during 5 h, and with twice-filtered seawater (TFSW, 0.45 µm and 0.22 µm), enabling the lugworms
228 to burry. The sediment was well mixed before the transfer in order to avoid air bubbles inclusions
229 between sediment grains. In the condition in which lugworms were supposed to experience an active
230 metabolic rate, around 30 of the collected individuals were transferred into centrifuge tubes filled
231 with TFSW only, where they were constantly trying to burry (no sand). Blanks were also made
232 for both conditions (centrifuge tubes without lugworms). Lugworms were acclimatized 24 hours
233 at the experimental temperature in order to allow them to burrow when possible and relax. For
234 each condition, centrifuge tubes were oxygenated using an air pump, and refilled with oxygenated
235 TFSW when needed. At this point, lugworms in the "active" condition experienced regularly extra
236 stress due to water movements. The oxygen content was then measured using a microelectrode
237 Unisense® OX500 coupled to a picoammeter (Unisense PA 2000, Denmark). The data acquisition
238 was performed using the software InstaCal® and the tubes were then rapidly hermetically closed
239 with Parafilm® M. For the 50 ml centrifuge tubes, measurement was renewed three times every 10
240 to 15 minutes after opening the Parafilm® M lid for a few seconds and homogenizing the water.
241 For the 5 ml tubes, only two measurements were made at the beginning of the experiment and
242 after 1 h given the low oxygen consumption observed. Before every measurement series, the whole
243 system was calibrated (measurements of 100% and 0% oxygenated TFSW) and the salinity of the
244 TFSW used for the experiment was measured using a refractometer. The temperature of the cold
245 room was followed throughout the duration of the experiment. After the experiment, lugworms
246 from the sand condition were sieved out of their tubes and maintained 24 h to allow gut contents
247 to be devoided prior to biometric measurements. All lugworms were then measured (trunk length
248 and total length) and weighed (wet weight).

249 *Experiment B: Reproductive data.* All oocytes were collected, from females that had been previ-
250 ously weighted and measured, in a 60 μm sieve, rinsed with TFSW and placed in a 5 ml Eppendorf
251 tube filled with TFSW (Table 2). A triplicate of 20 μL of the homogenized solution were then put
252 on a microscope slide and the oocytes were counted under the microscope. When fecundity was
253 estimated for each female, the supernatant was removed and the Eppendorf tubes were weighted
254 with and without oocytes.

255 *Experiment C: Growth experiment.* The growth experiment lasted for two months in a controlled
256 room (temperature, photoperiod) at the Wimereux Marine Station (University of Lille, France)
257 under a recirculating custom seawater system (Fig. 3). In the custom system, one aquarium
258 tray was dedicated to water filtering and two aquaria held the lugworm growing experiment. The
259 seawater, directly pumped from the sea, was kept several days in the filtering aquarium containing
260 fine and coarse filter foam, crushed pozzolana and oyster shells and kept in the dark (Fig. 3).
261 10% of the seawater contained in the two growing aquaria was renewed every day or every second
262 day with the water of the filtering aquarium. Two external filters (Eheim professional 4+ 250)
263 and pumps allowed the circulation and additional filtration of the seawater system (Fig. 3a). A
264 lightening system consisting in two light ramps (Alpheus Radiometrix 13C1001C) mimicking the
265 external light intensity and photoperiod was added to the system (Fig. 3a), air pumps (Air pump
266 8000 and Eheim 400 from Europrix ltd., not represented on Fig. 3) linked to home-made finely
267 punctured pipes allowed the oxygenation of the system. The temperature was kept around 15°C (\pm
268 1°C). Each of the two growing aquarium trays were holding each twice 3 boxes filled with sediment
269 burnt at 60°C during 24 h and lugworms (Fig. 3b). The first 3 boxes closer to the seawater arrival
270 were dedicated to the unfed condition, the next 3 to the fed condition. A small waterfall between
271 them prevented the seawater (and food) to circulate in the opposite direction of the main current,
272 thus no food could reach the unfed condition. The design of the boxes and of the separations
273 prohibited the worms to leave their box and to circulate from one condition to another condition
274 (Figs. 3a, b). All lugworms were measured and only individuals ranging from 0.4 cm to 1.6 cm of
275 trunk length were selected. Twelve batches of 30 individuals were made with the same size (trunk
276 length) range. Each batch was placed in a separated box within the experimental set up (Fig. 3b).
277 Feeding occurred twice at $t = 0$ and $t = 35$ days with yeast wastes (obtained from Brasserie du
278 pays Flamand ltd., a local brewery) inserted within the sediment with 20 ml syringes (between 1.8
279 and $3.6 \cdot 10^{10}$ cells added per box) (Olive et al., 2006). One batch of lugworms of each condition in
280 both aquaria was withdrawn at the beginning of the experiment, after 35 days and after 62 days,
281 kept 24 h in the cold room and weighted and measured.

282 *Data analyses.* All data analyses were performed on Matlab R2015b. For the oxygen consumption
283 experiment (Exp. A), for each measurement (blanks included), the associated percentage of oxygen

284 within the tube was calculated according to the Equation (2).

$$O_{2 \text{ measured}}(\%) = \frac{O_{2 \text{ measured}}(V) - O_{2 \text{ min}}(V)}{O_{2 \text{ max}}(V) - O_{2 \text{ min}}(V)} \cdot 100 \quad (2)$$

285 With $O_{2 \text{ measured}}(V)$ the oxygen measured, $O_{2 \text{ min}}(V)$ the oxygen measured for 0% of oxygen, and
286 $O_{2 \text{ max}}(V)$ the oxygen measured for 100% of oxygen. The oxygen content ($\mu\text{mol.L}^{-1}$) was then
287 calculated according to the temperature (T, in $^{\circ}\text{C}$), salinity (S, in ‰) and the water content of
288 each tube according to Aminot and K erouel (2004, see on pages 110-118). The blank effect was
289 deleted, and the individual oxygen consumption ($\mu\text{mol.h}^{-1}$) was then calculated as the inverse of
290 the slope of the linear regression of the evolution of the oxygen content over time. Both conditions
291 were analyzed together to consider an average level of activity.

292 For the reproduction data acquisition, the fecundity (F) was calculated for each female according
293 to Equation (3) (with n the mean of the three counts).

$$F = \frac{n}{4 \cdot 10^{-3}} \quad (3)$$

294 Since spawning happens only once a year for *A. marina*, the reproduction rate for each female
295 was calculated as the fecundity divided by the number of days in one year and plotted against the
296 female trunk length (uni-variate data). The wet weight of an egg was calculated as the total weight
297 of oocytes divided by fecundity (zero-variate data).

298 1.2.3. Parameters estimation

299 The parameters estimation of the DEB models was done using the covariation method described
300 by Lika et al. (2011), using the dataset shown in Table 3. The estimation was completed using the
301 package DEBtool (as described in Marques et al., 2018) on the software Matlab R2015b using both
302 a std-DEB model and an abj-DEB model, in order to select the best fit model and to compare the
303 parameter obtained with both models.

304 The parameter estimation procedures were evaluated by computing the Mean Relative Errors
305 (MRE), varying from 0, when predictions match data exactly, to infinity when they do not, and
306 the Symmetric Mean Square Errors (SMSE), varying from 0, when predictions match data exactly,
307 to 1 when they do not (<http://www.debtheory.org>).

308 1.3. Inferring environmental conditions from biological data and vice versa

309 1.3.1. Functional scaled response associated to growth data

310 The parameters of abj-model for *Arenicola marina* (best fit model), as well as two different
311 growth datasets, were used to validate the model and infer the environmental conditions (in terms
312 of food levels) of these datasets. The first growth dataset was taken from Beukema and De Vlas
313 (1979). It represents seasonal changes in mean individual dry weight (9-year averages) in small
314 lugworms from two populations of the Wadden Sea. The second dataset consists of the observations
315 of wet weight and trunk length of the experiment C. Since the results of the latest experiment
316 seemed to indicate that food was lacking from $t = 35$ days to $t = 62$ days and since no significant

317 difference between the two feeding conditions were observed, the abj-model applied in this study
318 was used to reconstruct the scaled functional response (f) as a proxy of food levels during the
319 whole experiment for the two conditions. Predictions on these different growth experiments were
320 made at one temperature but for feeding conditions varying from $f = 0.02$ to $f = 1$. The best
321 fit predictions were chosen as the ones presenting the smallest sum of squares of the differences
322 between observations and predictions.

323 1.3.2. Life cycle chronology under *in situ* environmental conditions

324 The abj-DEB model for *Arenicola marina* was used to reconstruct the chronology of the early
325 life stages of the species under the *in situ* environmental conditions of Wimereux (Eastern English
326 Channel, Hauts-de-France), as well as its growth in wet weight and trunk length, and compared
327 them with optimal food and temperature conditions ($f = 1$ and $T = 20$ °C).

328 *Local environmental conditions.* The *in situ* temperature of the year 2017 were taken from SOM-
329 LIT. As a first approximation, the scaled functional response f was guessed from monitoring of the
330 phytoplankton within the Eastern English Channel (Lefebvre et al., 2011) showing higher abun-
331 dances in spring and autumn, as generally observed in the North Atlantic temperate ocean (Miller
332 and Wheeler, 2012, Fig. 11.7).

333 *Chronology of the early life-stages and associated lengths.* The parameters of the abj-model pre-
334 viously estimated were used to predict age and length at trochophore larva stage, birth, meta-
335 morphosis and puberty under the non-optimal environmental conditions of Wimereux previously
336 defined.

337 *Growth predictions.* The evolution of the compartments of reserve, structure and reproduction
338 buffer from the fertilization to the lifespan a_m and further was calculated according to the equations
339 of Table 1. For each environmental condition, the ages for all the life stages were predicted as
340 previously and a temperature correction was applied when the temperature was different from 20
341 °C. The values of E , V and E_R over time were then converted into wet weight and/or physical
342 trunk length with the equations found in Table 1.

343 1.4. Comparison of the DEB parameters of *Arenicola marina* with other Lophotrochozoan species

344 The parameters found with the abj-DEB model for *Arenicola marina* were compared with the
345 ones found with the std-model, as well as with the parameters of other molluscs and annelid species.
346 The parameters collected were taken from the Add-my-Pet collection (AmP) (Marques et al., 2018)
347 using the function prtStat of the AmPtool package used on Matlab R2015b. All values were given
348 for a reference temperature T_{ref} of 20 °C. The most complete data set for molluscs is for the
349 gastropod *Lymnaea stagnalis* (completeness = 5). The maximum completeness value for annelids
350 in AmP is 2.8, and is found in two species of polychaetes and four species of clitellates. The least
351 complete data set for molluscs is for the symbiotic bivalve *Thyasira cf. gouldi* (completeness = 1.5)

352 and the least complete data set for annelids is for the polychaete *Capitella teleta* (completeness =
353 1.5).

354 Some of the primary parameters of the two models for *A. marina* were not compared given the
355 lack of data for these parameters (e.g. the searching rate $\{\dot{F}_m\}$, the digestion and the reproduction
356 efficiencies κ_X and κ_R), as in Kooijman and Lika (2014). The acceleration factor s_M of *A. marina*
357 was calculated as $s_M = L_j/L_b$, with L_b the structural length at birth and L_j the structural length at
358 the end of the metamorphosis, and compared with the one of other species. For the species showing
359 a metabolic acceleration ($s_M > 1$), the infinite length L_∞ was calculated as $L_\infty = L_m \cdot s_M$, with L_m
360 the maximum structural length ($L_m = \kappa \cdot \frac{\{p_{Am}\}}{[p_M]}$). The energy conductance after metamorphosis
361 v_j and the maximum assimilation rate after metamorphosis $\{p_{Am}\}_j$ were calculated as $v_j = v_b \cdot s_M$
362 and $\{p_{Am}\}_j = \{p_{Am}\}_b \cdot s_M$, with v_b the energy conductance at birth and $\{p_{Am}\}_b$ the maximum
363 assimilation rate at birth (Kooijman, 2014; Kooijman and Lika, 2014). All ten parameters, as well
364 as the expectations based on the general animal (Kooijman, 2010, Table 8.1), were represented as
365 functions of L_∞ for all the considered species.

366 2. Results

367 2.1. Parameter estimation

368 2.1.1. Parameters of the model

369 The completeness of the models was set at 4.2 following Lika et al. (2011) according to the
370 dataset used in the parameters estimation (Table 3). The implementation of the parameter es-
371 timation of the std-DEB model provided a Mean Relative Error (MRE) of 0.30 and Symmetric
372 Mean Square Error (SMSE) of 0.38 (Marques et al, 2018). The implementation of the parameter
373 estimation of the abj-DEB model provided a MRE of 0.23 and SMSE of 0.29. In addition to the
374 fact that the abj-model provided a better fit to the data set, it appears that the std-model largely
375 underestimates the age and length at birth, a_b and L_b (the relative errors, RE, are respectively
376 0.91 and 0.83), as well as the age when then trochophore larva appears, a_{tr} , (RE = 0.60). For both
377 models, the values of the fraction of the metabolized energy allocated to soma, κ , appeared equal
378 (Table 4). The specific somatic maintenance rate, $[p_M]$, and the maximum assimilation rate at
379 birth, $\{p_{Am}\}_b$, and at metamorphosis, $\{p_{Am}\}_j$, were respectively five, twenty and two times higher
380 with the std-model than with the abj-model. However, the maturation thresholds for the occurring
381 of the trochophore larva, E_H^{tr} , for birth, E_H^b , and for puberty, E_H^p , and the energy conductance at
382 metamorphosis, \dot{v}_j , appeared higher with the abj-model, that considered a metabolic acceleration
383 rate between birth and metamorphosis, s_M , around 11 (Table 4).

384 2.1.2. Observations vs predictions

385 *Zero-variate data.* For 9 of the 12 zero-variate observations of the estimation procedure with the
386 abj-model, the predicted values were close to the observed ones (RE \leq 0.27) (Table 5). The last
387 three predictions for the age at birth a_b , the age at puberty a_p and the total length at birth L_b

388 showed higher relative errors (RE \sim 0.65). The predictions obtained with the std-model estimation
389 procedure were overall less well adjusted to the zero-variate observations with 50% of the predictions
390 associated RE higher than 0.45 (Table 5). For instance, the age at birth a_b , the age when the
391 trochophore larva is first observed a_{tr} and the age at puberty a_p were highly underestimated with
392 the std-model estimation procedure (RE respectively of 0.91, 0.6 and 0.74), as well as the total
393 length at birth L_b and the length when the trochophore larva is first observed L_{tr} (RE respectively
394 of 0.83 and 0.45).

395 *Uni-variate data.* The RE of the uni-variate data set ranged from 0.06 to 0.41 with the abj-
396 DEB model, and from 0.08 to 0.42 with the std-DEB model, with, in both cases, the highest
397 values corresponding to the fit to the length-weight data collected on individuals of highly variable
398 reserve and reproduction buffer levels, and to the oxygen consumption data set (most scattered
399 values) (Figs. 4, 5, 6, 7). In both cases, the oxygen consumption increased with the increase of
400 temperature (Fig. 4). The values of the shape coefficients δ_M varied for *a priori* the same measure
401 of the trunk length between 0.14 and 0.20 with the abj-DEB model and between 0.09 and 0.13 with
402 the std-DEB model according to the authors (Fig. 7), which is due to the lack of rigid measurable
403 parts in *Arenicola marina* that could be used as a proxy for length.

404 2.2. Reconstruction of environmental conditions with the abj-model for *Arenicola marina* from bi- 405 ological data and vice versa

406 2.2.1. Scaled functional response

407 *From a field growth dataset.* The abj-model provided a good fit for the field growth data taken
408 from Beukema and De Vlas (1979) for the two studied sites (Fig. 8a). The values of the scaled
409 functional response f were shown to evolve on both sites during the year, with the highest values
410 during spring and late summer periods compared to winter period (Fig. 8a).

411 *From laboratory growth data.* Overall, the abj-model provided a good fit for the growth data
412 obtained in the laboratory (Exp. C), although growth was slightly underestimated between $t = 0$
413 and $t = 35$ d, and slightly overestimated between $t = 35$ and $t = 62$ d (Fig. 8b). The reconstruction
414 of the scaled functional response f provided indications on the fact that the food levels within the
415 sediment between $t = 35$ d and $t = 62$ d might have been really low and did not allow an optimal
416 growth.

417 2.2.2. Chronology and growth during the life cycle according to the environmental conditions

418 *In situ environmental conditions.* The seawater temperatures ranged from 5.5 to 20 °C at Wimereux,
419 with the highest temperature between July and September and the lowest temperature between
420 January and February (Fig.9a). The scaled functional response was supposed to range from 0.3 to
421 0.95 with higher values in spring and autumn and lower values in summer and winter (Fig.9b).

422 *Chronology of the first life stages.* The abj-model predicted an age at trochophore larva stage a_{tr}
423 of 10.3 days and an age at birth a_b (used as an approximation of the age at the first settlement)
424 of 15.5 days at Wimereux, considering the environmental conditions presented in Fig. 9 (Table
425 6), suggesting a first dispersal phase in between these two events of around 5 days. The age at
426 the end of metamorphosis a_j was predicted to be 208 days (a little less than 7 month) in local
427 environmental conditions, which means around mid April for a spawning period in mid September.
428 The age and trunk length at puberty of the lugworms of Wimereux, a_p and TL_p , were predicted
429 to be respectively 373.2 days and 3.5 cm.

430 *Wet weight and trunk length growth predictions according to the environmental conditions.* The
431 total wet weight of *Arenicola marina* (considering the structure, reserve and reproduction buffer
432 compartments) predicted by the model at the maximum age a_m was around 20 times superior in
433 optimal conditions ($f = 1$ and $T = 20^\circ\text{C}$, around 400 g) compared to *in situ* conditions recorded
434 at Wimereux ($f = 0.4$ and $T = 13^\circ\text{C}$, around 20 g) (Fig. 10). The total trunk length of *A. marina*
435 predicted by the model was more than twice superior in optimal conditions ($f = 1$ and $T = 20^\circ\text{C}$,
436 around 33 cm) than in the environmental conditions recorded at Wimereux ($f = 0.4$ and $T = 13^\circ\text{C}$,
437 around 14 cm) (Fig.11).

438 2.3. Comparison of the abj-DEB parameters of *Arenicola marina* with other Lophotrochozoan species

439 In annelids and molluscs, the maximum assimilation rate, $\{\dot{p}_{Am}\}$, increased with the maxi-
440 mum structural length as expected, and more markedly after metamorphosis and the associated
441 metabolic acceleration phase (Fig. 12). The values for *Arenicola marina* with the abj-model ap-
442 peared lower than those of most of the other polychaetes and clitellates species before and after
443 metamorphosis, except for the values of *Urechis caupo* (echiurian species), the only other annelid
444 species for which an abj-model was applied.

445 The value of the maximum assimilation rate after metamorphosis, $\{\dot{p}_{Am}\}_j$, of *A. marina* with
446 both models was close to the one expected for the generalized animal, and followed the tendency
447 found in most of the others mollusc species, which was not the case for the other polychaetes species,
448 mostly showing higher values. The allocation fraction to soma, κ , was higher for *A. marina* (\sim
449 0.92) than the one expected for the generalized animal (0.8), and did not appear inconsistent with
450 the values of κ calculated in molluscs species (Fig. 12). The energy conductance value, \dot{v} , for *A.*
451 *marina* appeared lower in the abj- than in the std-model before metamorphosis, but the opposite
452 happened after metamorphosis, where the abj-model's value was higher than the generalized animal
453 but closer to molluscs' values. The specific somatic maintenance costs values, $[\dot{p}_M]$, of *A. marina*
454 were much lower than those predicted for most of the other species of annelids (except for *Urechis*
455 *caupo*) but were close to the one of the generalized animal and are consistent with the values for
456 the molluscs species (Fig. 12). The value of the costs of structure, $[E_G]$, of *A. marina* appeared
457 equal to those of the other annelids' and most of the molluscs' species (Fig. 12). The value of the

458 maturity maintenance rate coefficient, k_j , of *A. marina* was equal to those of the other annelids'
459 and of most of the molluscs' species (Fig. 12). The values of the maturity thresholds for birth,
460 metamorphosis and puberty, E_H^b , E_H^j , and E_H^p , of the abj-model for *A. marina* were lower than
461 those of the generalized animal but similar to most of the mollusc species' values (Fig. 12).

462 3. Discussion

463 In the present study, we successfully estimated the parameters of both a std- and an abj-DEB
464 model for the lugworm *Arenicola marina*, combining the use of literature, experimental and field
465 data. We found that the abj-model was more appropriate for modelling *A. marina*'s energy budget
466 and life cycle and implemented it under field conditions to reconstruct feeding levels as well as *A.*
467 *marina*'s growth and life cycle chronology.

468 3.1. Physiological implications of the std- and the abj- parameter estimation results

469 Major differences in the organisms physiology were implied by the parameter results obtained
470 with a faster metabolism for *Arenicola marina* with a std-DEB model compared to an abj-DEB
471 model. Indeed, $\{\dot{p}_{Am}\}_b$, $\{\dot{p}_{Am}\}_j$, $[\dot{p}_M]$ and \dot{v}_b appeared higher with the std- parameter estimation,
472 and \dot{v}_j higher with the abj- parameter estimation. First, a higher value of the maximum assim-
473 ilation rate $\{\dot{p}_{Am}\}$ implies a higher value of the assimilation flux from the same amount of food,
474 and a higher value of the energy conductance \dot{v} implies a larger mobilization flux (Agüera et al.,
475 2015). The reserve capacity $[E_m]$, defined by the ratio $[E_m] = \{\dot{p}_{Am}\} / \dot{v}$ (Montalto et al., 2014) was
476 found to be 16766 J.cm⁻³ with the std- parameter estimation compared to 1177 J.cm⁻³ with the
477 abj- parameter estimation (considering a temperature of 20°C). In comparison, $[E_m]$ values for ac-
478 celerating molluscs species were estimated around 4500 J.cm⁻³ and $[E_m]$ values for non-accelerating
479 molluscs species were estimated around 11600 J.cm⁻³ (Add-my-Pet collection consulted in Novem-
480 ber 2018). Second, a higher value of the volume-specific maintenance costs, $[\dot{p}_M]$, implies a higher
481 level of energy needed for the same amount of structure acquired. The comparison of the parame-
482 ter estimation of the abj- and std- models therefore resulted on the one hand, with the parameter
483 estimation of the std-model, in one organism able to store more energy in the reserve compart-
484 ment, but also using more energy for the maintenance of its structure, and on the other hand,
485 with the parameter estimation of the abj-model, in one organism able to store less energy in the
486 reserve compartment, but using less energy for the maintenance of its structure. Indeed, although
487 the predictions of the std- and abj- versions of the model were quite similar (except for the early
488 life-stages predictions), they implied really different bioenergetics in two kinds of organisms storing
489 and using energy differently.

490 3.2. Implications of using an abj-model for *Arenicola marina* in relation with its biology and ecology

491 For *Arenicola marina*, the abj-model gave better fit results than the std-model (smaller MRE
492 and SMSE), even when only few observations within the data set accounted for the acceleration

493 period (only the zero-variate observations a_j and L_j were added, but no uni-variate observations
494 made between birth and metamorphosis). The presence of a metabolic acceleration between birth
495 and metamorphosis in *A. marina* might be related to its benthopelagic life cycle. Indeed, acceler-
496 ating species have longer incubation time (before birth) than non-accelerating species (Kooijman,
497 2014; Kooijman et al., 2011), which might be linked to the presence of a larval dispersal phase, since
498 a lower metabolism (in comparison with a non-accelerating species, or with juvenile or adult from
499 the same species) allows for more dispersal time, especially when dispersal rate mainly depends
500 on passive water transport (Kooijman, 2014). This seems in accordance with the presence of a
501 dispersal phase happening before birth for *A. marina* and with the fact that predictions of a_{tr} and
502 a_b of the std- model presented in this study appeared much smaller than observations, compared to
503 predictions made by the abj-model. In lugworms, the gradual change of feeding behaviour between
504 the first feeding at birth, the temporary settlement between birth and metamorphosis, and the
505 semi-permanent settlement after metamorphosis on the foreshores inhabited by adults (Farke and
506 Berghuis, 1979a, b) might be a mechanism of the increase of the metabolic acceleration s_M , also
507 increasing the resulting specific assimilation rate (since $\{\dot{p}_{Am}\}_j = s_M \cdot \{\dot{p}_{Am}\}_b$) of the individual.
508 The increase of the organic matter concentration within the water column during spring (spring
509 blooms), before the second dispersal phase when metamorphosis is almost completed, might also
510 play a role in the increase of the specific assimilation rate, increasing the amount of food available
511 for the same feeding effort.

512 3.3. Phylogenetic implications of the use of abj-DEB models for polychaetes

513 The metabolic acceleration rate value for *A. marina* (~ 11) falls in the range of what can be
514 found in mollusc species (for more than 95% of the mollusc species, $1 \leq s_M \leq 27$ in the AmP
515 database), which seems consistent with the fact that polychaetes and molluscs both belong to the
516 Lophotrochozoan clade, having both a common trochophore larval stage after the embryogenesis.
517 However, although all annelids are part of the Lophotrochozoan clade, they do not all share the
518 presence of at least one larval dispersal phase during their life cycle, and therefore, might not
519 all experience a metabolic acceleration during their life cycle. As an example, clitellates have a
520 direct development with no larval phase (related to their terrestrial habitat) and std-models might
521 show better fit for these species that may not experience a metabolic acceleration during their life
522 cycle. From an evolutionary point of view, metabolic acceleration might first have been common
523 to all Lophotrochozoans and secondarily lost in clitellate species (as suggested by Marques et al.,
524 2018, for other taxa). Nevertheless, since some species with no larval phase might also experience
525 a metabolic acceleration (Kooijman, 2014), and since metabolic acceleration seem common to a
526 large part of the species belonging to the Lophotrochozoan clade (Kooijman, 2014; Marques et
527 al., 2018), a comparison of the use of both abj- and std- models for clitellate species should be
528 considered.

529 3.4. Energy budget and *in situ* life cycle predictions

530 The predictions on the chronology of *Arenicola marina*'s life cycle stages under the *in situ*
531 environmental conditions met at Wimereux (metamorphosis completed at around 7 months, in
532 mid April) seemed in accordance with observations made by De Cubber et al. (2018), who spotted
533 the first recruits of the species (e.g. juveniles after metamorphosis) in May at the same site.
534 This would suggest a second dispersal period of less than one month if lugworms migrate after
535 metamorphosis. Moreover, the age and length at puberty of the lugworms at the Wimereux site
536 were predicted with the abj-model to be respectively 373.2 days and 3.5 cm, which is close to the
537 observations made by De Cubber et al. (2018) with a length at first spawning (after the acquisition
538 of maturity) of 3.8 cm and an age of 1.5 to 2.5 years. Newell (1949, 1948) reported the presence
539 of *A. marina* metatrochophore larvae close to birth (and thus close to the first settlement stage)
540 with 3 to 4 setigers and around 0.034 cm of length around 2 to 3 weeks after the occurrence of the
541 spawning event at Whistable (UK) (limit between the English Channel and the North Sea). His
542 observations also seem in accordance with the abj-model predictions. Indeed, the age and length at
543 birth predictions at Wimereux in October were of 15.5 days and 0.034 cm. Since temperatures are
544 lower in November in the English Channel and even lower in the North Sea, birth might have been
545 slightly delayed in their study and their observations seem to be in accordance with the abj-model
546 implemented in our study. Observations of post-larvae in mucus tubes were commonly made on
547 fucus and pebbles areas until the end of February (Benham, 1893; Newell, 1949, 1948) and up to
548 April in some cases (Newell, 1949). First settlements of juveniles on adult grounds were reported
549 by Newell (1949, 1948) at the end of April or beginning of May, which is in accordance with our
550 model predictions (after the age at metamorphosis, which is around 5 months-old) and correspond
551 to a dispersal period after metamorphosis of a maximum of one month.

552 The biggest individuals of *A. marina* collected at the studied sites might give indications on the
553 *in situ* environmental conditions met by the lugworms on these sites. Indeed, at Wimereux, the
554 heaviest individual collected by the authors between 2015 and 2018 weighted 10 g and the longest
555 one measured 15.2 cm of trunk length (data not shown), which is in accordance with the length and
556 weight predicted by the abj-model for *Arenicola marina* at an age of 5 to 6 years old (age of the last
557 cohort calculated by De Cubber et al. (2018)) for $f = 0.4$ and $T = 13^{\circ}\text{C}$. At Le Touquet (Eastern
558 English Channel, De Cubber et al., 2018), the heaviest individual collected weighted 53.1 g and
559 the longest one measured 20.2 cm of trunk length (data no shown), and at Fort Mahon (Eastern
560 English Channel, De Cubber et al., 2018), the heaviest individual collected weighted 26 g and the
561 longest one measured 18.4 cm of trunk length (data not shown). Since no major difference between
562 the seawater temperature at the three different sites exist, the main difference was possibly the food
563 availability. The comparison of these biometric values with the ones predicted by the abj-model
564 (around 600 g of maximum wet weight and 35 cm of maximum trunk length for $f = 1$ and $T =$
565 13°C) seems to indicate that f was higher at Le Touquet and Fort Mahon compared to Wimereux.

566 In the different sites of the Eastern English Channel cited previously, De Cubber et al. (2018)
567 showed that the lugworms' recreational harvest in 2017 removed more than 500 000 lugworms and
568 represented a total retail value of around 232 447 euros. The need for implementing management
569 measures was also evidenced for at least one beach by these authors. Knowing the food levels of the
570 different sites might then enable predictions with the abj-model on the *in situ* ages and lengths at
571 puberty, which could help managers to implement relevant regulations if needed such as a relevant
572 harvest minimum size limit on the different sites showing highly variable food levels and maximum
573 lengths and weights.

574 3.5. Possible future extensions of the model

575 In order to provide the best model possible for *Arenicola marina* further adjustments could be
576 implemented linked to the species life cycle and habitats. First, defining the temperature tolerance
577 range of the species could improve the abj-model by applying better temperature corrections.
578 Growth experiments from Farke and Berghuis (1979) seem to point out a higher boundary of
579 the temperature tolerance range T_H around 25 °C. Other studies suggest a lower boundary of
580 the temperature tolerance range T_L under 5°C (Sommer et al., 1997; Wittmann et al., 2008),
581 but no Arrhenius temperatures beyond the temperature tolerance (T_{AH} and T_{AL}) range could
582 be calculated yet. Further experiments on growth or respiration under temperatures beyond the
583 temperature tolerance range could be performed to define T_{AH} and T_{AL} and thus improve the
584 temperature correction.

585 During their life cycle, the different stages of *A. marina* inhabit different marine habitats with
586 different ranges of temperature variation. From the metatrochophore to the post-larval stage the
587 lugworms inhabit the subtidal area where seawater temperature does not fluctuate that much daily,
588 compared to the intertidal areas inhabited by the juveniles and adults, where temperature can
589 change dramatically during one day. As an example, a variation of 15°C was recorded within
590 the sediment at the Wimereux site in November 2017 (Fig. 13). In this study, the Arrhenius
591 temperature was calculated from the oxygen consumption rate of juveniles living on the upper
592 shore. We hypothesize that a different Arrhenius temperature may exist for the larval and post-
593 larval stages living in habitats with a more stable temperature, as suggested by Kooijman (2010).
594 Further experiments could be implemented on larvae in order to record physiological rates and
595 estimate their Arrhenius temperature.

596 Monaco and McQuaid (2018) highlighted the interest of adding to the temperature correction
597 an aerial exposure term M_d (linked to tidal height and the position of organisms on the shore) in
598 foreshore habitats showing wide fluctuations in temperature and desiccation. Given the intense
599 variations experienced by juvenile and adult lugworms (Fig. 13), it might be interesting to add an
600 aerial exposure term for the species. Indeed, the underestimation of growth by the model compared
601 to our observation of growth of juveniles in the laboratory (Exp. C) might be linked to the fact
602 that no tide was simulated and lugworms stayed immersed during all the experiment time, without

603 the stress brought by high temperature variations and aerial exposure. However, it was found that
604 lugworms gradually migrate down the shore while growing (De Cubber et al., 2018), so the aerial
605 exposure correction, if implemented, should gradually decrease during the life cycle of the organism
606 as well.

607 DEB models as implemented here enable to reconstruct the growth and the reproduction of
608 a species at the individual level. However, in order to be used in a population context, DEB
609 theory can be associated to individual-based models (IBM) in order to explore properties of both
610 individual life-history traits and population dynamics (Bacher and Gangnery, 2006; Martin et al.,
611 2012). The association of the abj-model developed here, and providing predictions on the duration
612 of the larval dispersal phase, with biophysical larval dispersal models (Nicolle et al., 2017) could
613 also allow the understanding of the populations' connectivity in the area and thus give valuable
614 information for the conservation of the species.

615 Acknowledgements

616 We would like to thank D. Menu for his help in the design and creation of the growth system, and
617 V. Cornille for his technical support on the field. This work was partly funded by the University of
618 Lille and CNRS. We are grateful to Europe (FEDER), the state and the Region-Hauts-de-France for
619 funding the experimental set up and T. Lancelot (research assistant) through the CPER MARCO
620 2015 - 2020. L. De Cubber is funded by a PhD studentship from the University of Lille. Finally
621 we would like to thank Starrlight Augustine and an anonymous reviewer for their comments that
622 help improving this manuscript.

623 References

- 624 Agüera, A., Collard, M., Jossart, Q., Moreau, C., Danis, B., 2015. Parameter estima-
625 tions of Dynamic Energy Budget (DEB) model over the life history of a key antarctic
626 species: The antarctic sea star *Odontaster validus* (Koehler, 1906). PLoS One 10, 1–23.
627 <https://doi.org/10.1371/journal.pone.0140078>
- 628 Aminot, A., Kerouel, R., 2004. Hydrologie des écosystèmes marins; paramètres et analyses,
629 Ifremer. ed.
- 630 Bacher, C., Gangnery, A., 2006. Use of dynamic energy budget and individual based models
631 to simulate the dynamics of cultivated oyster populations. J. Sea Res. 56, 140–155.
- 632 Benham, W.B., 1893. The Post-Larval Stage of *Arenicola marina*. J. Mar. Biol. Assoc.
633 United Kingdom 3, 48–53. <https://doi.org/10.1017/S0025315400049559>
- 634 Beukema, J.J., De Vlas, J., 1979. Population parameters of the lugworm *Arenicola ma-*
635 *rina* living on tidal flats in the Dutch Wadden Sea. Netherlands J. Sea Res. 13, 331–353.
636 [https://doi.org/10.1016/0077-7579\(79\)90010-3](https://doi.org/10.1016/0077-7579(79)90010-3)

637 Blake, R.W., 1979. Exploitation of a natural population of *Arenicola marina* (L.) from the
638 North-East Coast of England. J. Appl. Ecol. 16, 663–670. <https://doi.org/10.2307/2402843>

639 Cadman, P., Nelson-Smith, A., 1990. Genetic evidence for two species of lugworm (*Arenicola*)
640 in South Wales. Mar. Ecol. Prog. Ser. 64, 107–112. <https://doi.org/10.3354/meps064107>

641 Cadman, P.S., Nelson-Smith, A., 1993. A new species of lugworm: *Arenicola defodiens* sp.
642 nov. Mar. Biol. Ass. U.K 73, 213–223. <https://doi.org/10.1017/S0025315400032744>

643 De Cubber, L., Lefebvre, S., Fisseau, C., Cornille, V., Gaudron, S.M., 2018. Linking life-
644 history traits, spatial distribution and abundance of two species of lugworms to bait col-
645 lection: A case study for sustainable management plan. Mar. Environ. Res. <https://doi.org/10.1016/j.marenvres.2018.07.009>

647 De Wilde, P.A.W.J., Berghuis, E.M., 1979. Laboratory experiments on growth of juvenile
648 lugworms, *Arenicola marina*. Netherlands J. Sea Res. 13, 487–502. [https://doi.org/10.1016/0077-7579\(79\)90020-6](https://doi.org/10.1016/0077-7579(79)90020-6)

650 Farke, H., Berghuis, E.M., 1979a. Spawning, larval development and migration of *Arenicola*
651 *marina* under field conditions in the western Wadden sea. Netherlands J. Sea Res. 13,
652 529–535.

653 Farke, H., Berghuis, E.M., 1979b. Spawning, larval development and migration behaviour of
654 *Arenicola marina* in the laboratory. Netherlands J. Sea Res. 13, 512–528.

655 Galasso, H.L., Richard, M., Lefebvre, S., Aliaume, C., Callier, M.D., 2018. Body size and
656 temperature effects on standard metabolic rate for determining metabolic scope for activity of
657 the polychaete *Hediste (Nereis) diversicolor*. PeerJ 1–21. <https://doi.org/10.7717/peerj.5675>

658 Kooijman, S.A.L.M., 2014. Metabolic acceleration in animal ontogeny: An evolutionary
659 perspective. J. Sea Res. 94, 128–137. <https://doi.org/10.1016/j.seares.2014.06.005>

660 Kooijman, S.A.L.M., 2010. Dynamic energy budget theory for metabolic organisation. Cam-
661 bridge University Press.

662 Kooijman, S.A.L.M., Lika, K., 2014. Comparative energetics of the 5 fish classes on the basis
663 of dynamic energy budgets. J. Sea Res. 94, 19–28. <https://doi.org/10.1016/j.seares.2014.01.015>

665 Kooijman, S.A.L.M., Pecquerie, L., Augustine, S., Jusup, M., 2011. Scenarios for accel-
666 eration in fish development and the role of metamorphosis. J. Sea Res. 66, 419–423.
667 <https://doi.org/10.1016/j.seares.2011.04.016>

668 Kristensen, E., 1981. Direct measurement of ventilation and oxygen uptake in three species
669 of tubicolous polychaetes (*Nereis* spp.). *J. Comp. Physiol. B Biochem. Syst. Environ.*
670 *Physiol.* 145, 45–50.

671 Lefebvre, A., Guiselin, N., Barbet, F., Artigas, F.L., 2011. Long-term hydrological and
672 phytoplankton monitoring (1992 – 2007) of three potentially eutrophic systems in the eastern
673 English Channel and the Southern Bight of the North Sea. *ICES J. Mar. Sci.* 68, 2029–2043.

674 Lika, K., Kearney, M.R., Freitas, V., van der Meer, J., Wijsman, J.W.M., Pecquerie, L.,
675 Kooijman, S.A.L.M., 2011. The 'covariation method' for estimating the parameters of the
676 standard Dynamic Energy Budget model I: Philosophy and approach. *J. Sea Res.* 66,
677 270–277. <https://doi.org/10.1016/j.seares.2011.07.010>

678 Llandres, A.L., Marques, G.M., Maino, J.L., Kooijman, S.A.L.M., Kearney, M.R., Casas, J.,
679 2015. A dynamic energy budget for the whole life-cycle of holometabolous insects. *Ecol.*
680 *Monogr.* 85, 353–371. <https://doi.org/10.1890/14-0976.1>

681 Mangum, C.P., Sassaman, C., 1969. Temperature sensitivity of active and resting metabolism
682 in a polychaetous annelid. *Comp. Biochem. Physiol.* 30, 111–116.

683 Marques, G.M., Augustine, S., Lika, K., Pecquerie, L., Domingos, T., Kooijman, S.A.L.M.,
684 2018. The AmP project: Comparing species on the basis of dynamic energy budget parame-
685 ters. *PLoS Comput. Biol.* 14, 1–23. <https://doi.org/10.1371/journal.pcbi.1006100>

686 Martin, B.T., Zimmer, E.I., Grimm, V., Jager, T., 2012. Dynamic Energy Budget theory
687 meets individual-based modelling: A generic and accessible implementation. *Methods Ecol.*
688 *Evol.* 3, 445–449. <https://doi.org/10.1111/j.2041-210X.2011.00168.x>

689 Miller, C.B., Wheeler, P.A., 2012. *Biological oceanography*, 2nd ed.

690 Monaco, C.J., McQuaid, C.D., 2018. Applicability of Dynamic Energy Budget (DEB) models
691 across steep environmental gradients. *Sci. Report* 8, 16384. [https://doi.org/10.1038/s41598-](https://doi.org/10.1038/s41598-018-34786-w)
692 [018-34786-w](https://doi.org/10.1038/s41598-018-34786-w)

693 Montalto, V., Palmeri, V., Rinaldi, A., Kooijman, S.A.L.M., Sarà, G., 2014. Dynamic energy
694 budget parameterisation of *brachidontes pharaonis*, a lessepsian bivalve in the Mediterranean
695 Sea. *J. Sea Res.* <https://doi.org/10.1016/j.seares.2014.05.007>

696 Newell, G.E., 1949. The later larval life of *Arenicola marina*. *J. Mar. Biol. Assoc. UK* 28,
697 635–639. <https://doi.org/https://doi.org/10.1017/S0025315400023456>

698 Newell, G.E., 1948. A contribution to our knowledge of the life history of *Arenicola marina* L.
699 *J. Mar. Biol. Assoc. UK* 27, 554–580. <https://doi.org/10.1017/S0025315400056022>

700 Nicolle, A., Moitié, R., Ogor, J., Dumas, F., Foveau, A., Foucher, E., Thiébaud, E., 2017.
701 Modelling larval dispersal of *Pecten maximus* in the English Channel: a tool for the spatial
702 management of the stocks. ICES J. Mar. Sci. 74, 1812–1825. [https://doi.org/10.1093/](https://doi.org/10.1093/icesjms/fsw207)
703 [icesjms/fsw207](https://doi.org/10.1093/icesjms/fsw207)

704 Norin, T., Malte, H., 2011. Repeatability of standard metabolic rate , active metabolic
705 rate and aerobic scope in young brown trout during a period of moderate food availability
706 1668–1675. <https://doi.org/10.1242/jeb.054205>

707 Olive, P.J.W., Craig, S., Cowin, P.B.D., 2006. Aquaculture of marine worms. US 7,004,109
708 B2.

709 Reise, K., 1985. Tidal flat ecology - An experimental approach to species interactions, Eco-
710 logical Studies.

711 Reise, K., Simon, M., Herre, E., 2001. Density-dependent recruitment after winter distur-
712 bance on tidal flats by the lugworm *Arenicola marina*. Helgol. Mar. Res. 55, 161–165.
713 <https://doi.org/10.1007/s101520100076>

714 Rousselot, M., Delpy, E., La Rochelle, C.D., Lagente, V., Pirow, R., Rees, J.F., Hagege,
715 A., Le Guen, D., Hourdez, S., Zal, F., 2006. *Arenicola marina* extracellular hemoglobin:
716 A new promising blood substitute. Biotechnol. J. 1, 333–345. [biot.200500049](https://doi.org/10.1002/
717 <a href=)

718 Sommer, A., Klein, B., Pörtner, H.-O., 1997. Temperature induced anaerobiosis in two pop-
719 ulations of the polychaete worm *Arenicola marina* (L.). Journal of Comparative Physiology,
720 167: 25-35. 25–35. <https://doi.org/doi:10.2514/6.1965-1209>

721 Van Der Meer, J., 2006. An introduction to Dynamic Energy Budget (DEB) models with
722 special emphasis on parameter estimation. J. Sea Res. 56, 85–102. [j.seares.2006.03.001](https://doi.org/10.1016/
723 <a href=)

724 Van Der Veer, H.W., Cardoso, J.F.M.F., Van Der Meer, J., 2006. The estimation of
725 DEB parameters for various Northeast Atlantic bivalve species. J. Sea Res. 56, 107–124.
726 <https://doi.org/10.1016/j.seares.2006.03.005>

727 Watson, G.J., Murray, J.M., Schaefer, M., Bonner, A., 2017. Bait worms: a valuable and
728 important fishery with implications for fisheries and conservation management. Fish Fish.
729 18, 374–388. <https://doi.org/10.1111/faf.12178>

730 Watson, G.J., Williams, M.E., Bentley, M.G., 2000. Can synchronous spawning be predicted
731 from environmental parameters? A case study of the lugworm *Arenicola marina*. Mar. Biol.
732 136, 1003–1017. <https://doi.org/10.1007/s002270000283>

733 Wittmann, A.C., Schröer, M., Bock, C., Steeger, H.U., Paul, R.J., Pörtner, H.O., 2008. In-
734 dicators of oxygen- and capacity-limited thermal tolerance in the lugworm *Arenicola marina*.
735 Clim. Res. 37, 227–240. <https://doi.org/10.3354/cr00763>

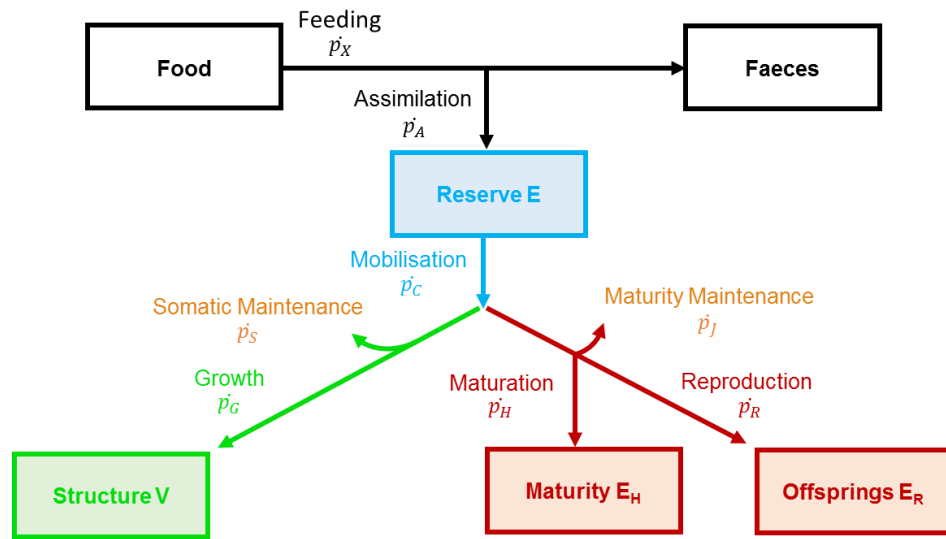


Figure 1: Schematic representation of DEB model and associated state variables and fluxes, adapted from Kooijman (2010). Boxes are the state variables: 1) reserve E (J); 2) the structural volume, V (cm^3); 3) the cumulated energy invested in Maturity, E_H (J) or in reproduction E_R (J). Arrows are energy flows in $\text{J}\cdot\text{d}^{-1}$. Details of \dot{p}_X , \dot{p}_A , \dot{p}_C , \dot{p}_S , \dot{p}_G , \dot{p}_J , \dot{p}_H and \dot{p}_R are given in Table 1.

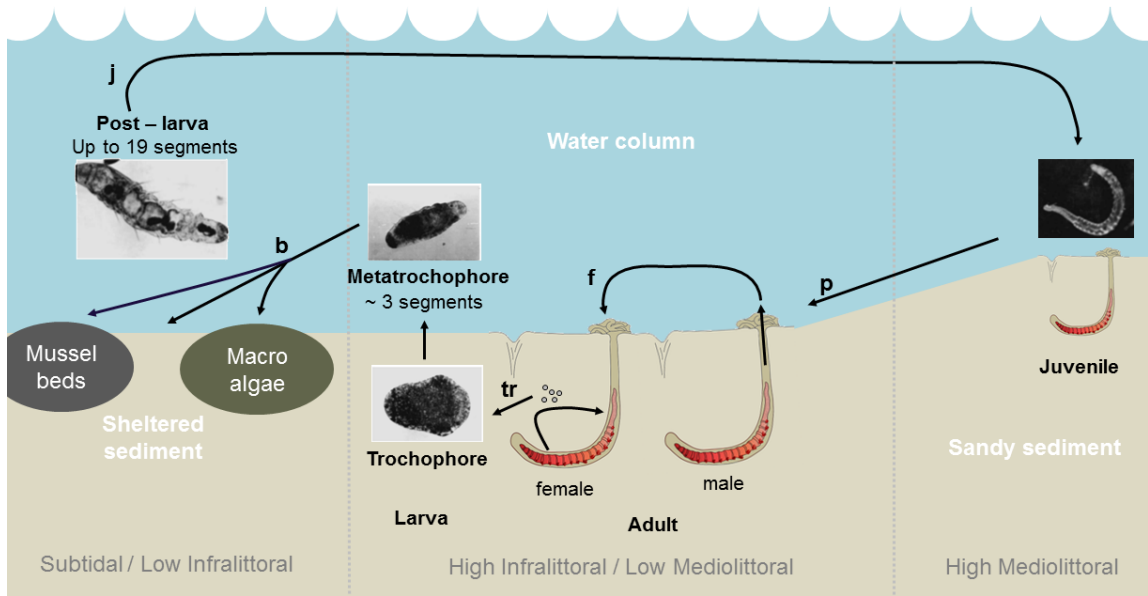


Figure 2: Life cycle of *Arenicola marina* and associated habitats. f stands for fertilization; tr for when the trochophore larva appears; b for birth (e.g. first feeding, as described in the DEB theory); j for the end of metamorphosis; and p for puberty. Adapted from Farke and Berghuis (1979a, 1979b), Reise (1985) and Reise et al. (2001). Pictures of the different life stages of *A. marina* are taken from Farke and Berghuis (1979a).

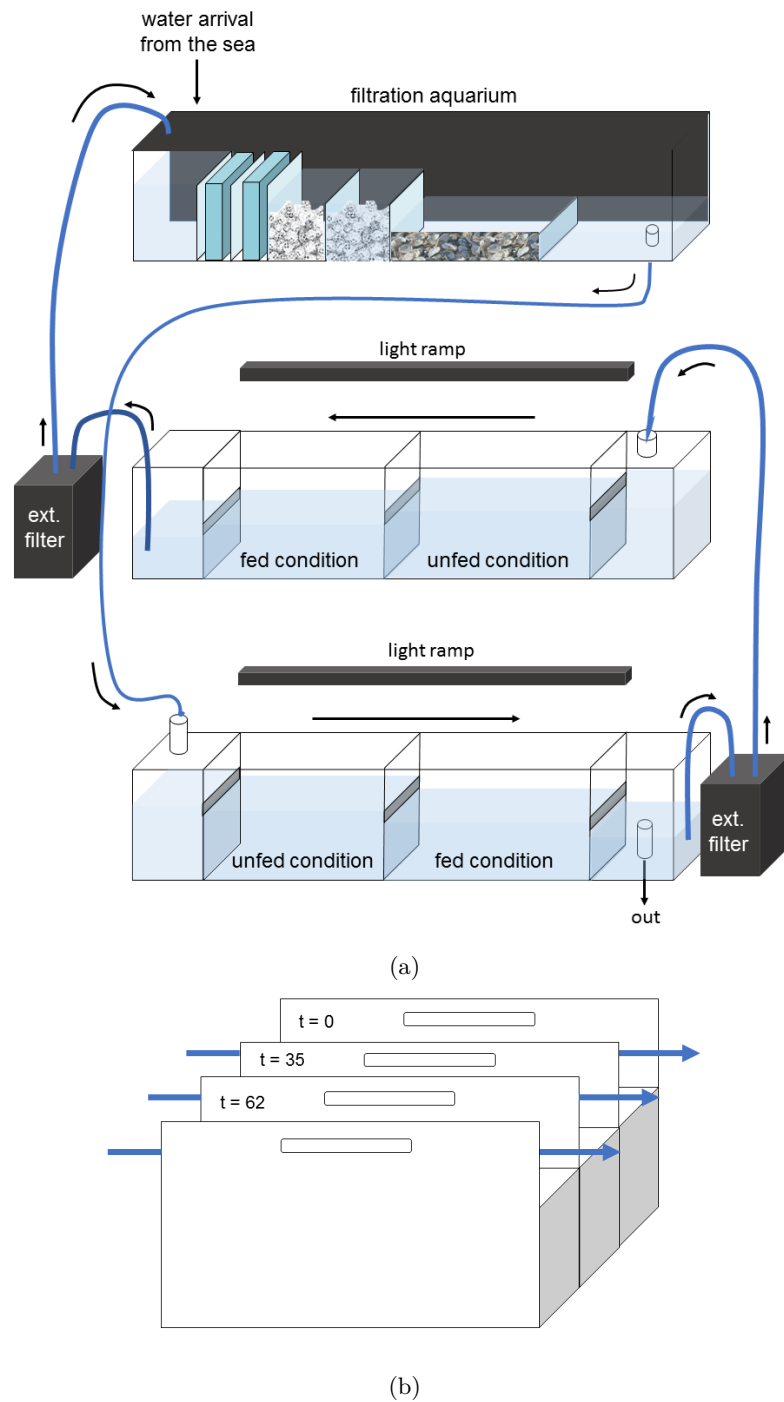


Figure 3: Circulation, filtration of seawater and lightening (a) and boxes (b) of the custom *Arenicola marina* growing system with recirculating seawater (Experiment C). The filtration aquarium tray (a, top aquarium) contained (from left to right): fine and coarse filter foam, crushed pozzolana and oyster shells. The boxes (b) were placed in each of the fed and unfed condition in the remaining aquarium trays and removed at $t = 0$ (first feeding of the fed condition), $t = 35$ and $t = 62$ days. The light ramps consisted in Alpheus Radiometrix 13C1001C, and the external (ext.) filters in Eheim professional 4+ 250. The oxygenation ramps placed in the last two aquarium trays are not represented.

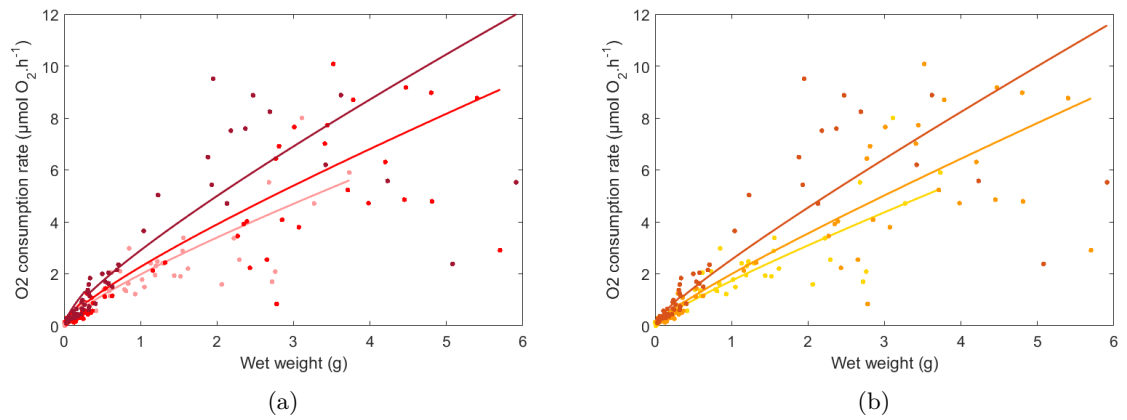


Figure 4: Data (dots) and predictions (lines) of the oxygen consumption of the abj-DEB model (a) and the std-DEB model (b) of *Arenicola marina* measured by the authors (Exp. A) as a function of wet weight at three different temperatures (from light to dark red: 12, 15 and 20.5°C). The respective relative errors from 12 to 20.5°C were 0.29, 0.38 and 0.40 with the abj-model (b) and 0.28, 0.33, and 0.38 with the std-model (b).

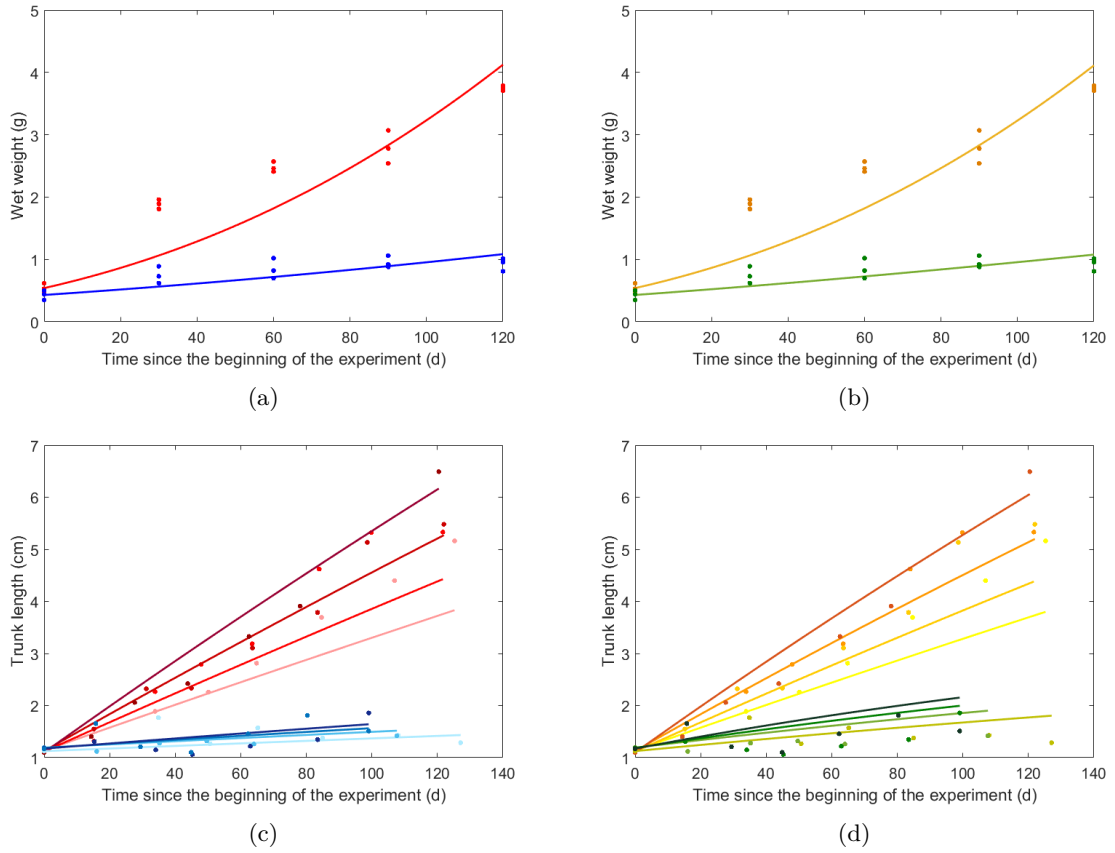
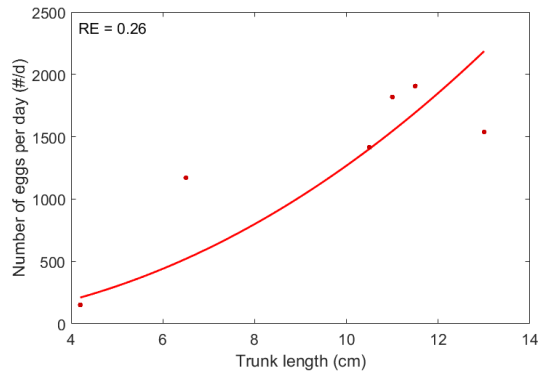
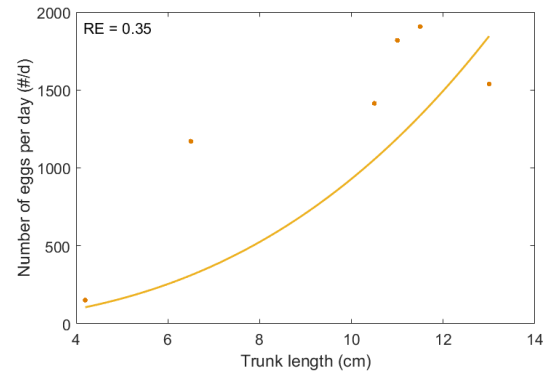


Figure 5: Data (dots) and predictions (lines) of the growth of *Arenicola marina* juveniles in wet weight (a,b) and in trunk length (c,d) using both an abj-DEB model (a,c) and a std-DEB model (b,d). Data from (a,b) was taken from Olive et al.(2006). *A. marina* was reared in fed (red and orange) and unfed (blue and green) conditions between 12 and 20°C. The respective relative errors (RE) for the growth curves in fed and unfed conditions were 0.19 and 0.15 (a) 0.18 and 0.15 (b). Data from (c,d) were taken from De Wilde and Berghuis (1979). *A. marina* was reared in fed (red and orange) and unfed (blue and green) conditions at four different temperatures (from light to dark: 5, 10, 15 and 20°C). The respective (RE) for the growth curves in fed conditions at 5, 10, 15 and 20°C were 0.15, 0.17, 0.07 and 0.13 with the abj-model (c) and 0.16, 0.18, 0.08 and 0.12 with the std-model (d). The respective RE for the growth curves in unfed conditions at 5, 10, 15 and 20°C were 0.11, 0.06, 0.13 and 0.12 with the abj-model (c) and 0.17, 0.19, 0.23 and 0.24 with the std-model (d).



(a)



(b)

Figure 6: Data (dot) and prediction (line) of the reproduction rate of *Arenicola marina* collected by the authors (Exp. B) (Eastern English Channel, France, see Table 2) as a function of trunk length using both an abj-DEB model (a) and a std-DEB model (b). RE stands for relative error.

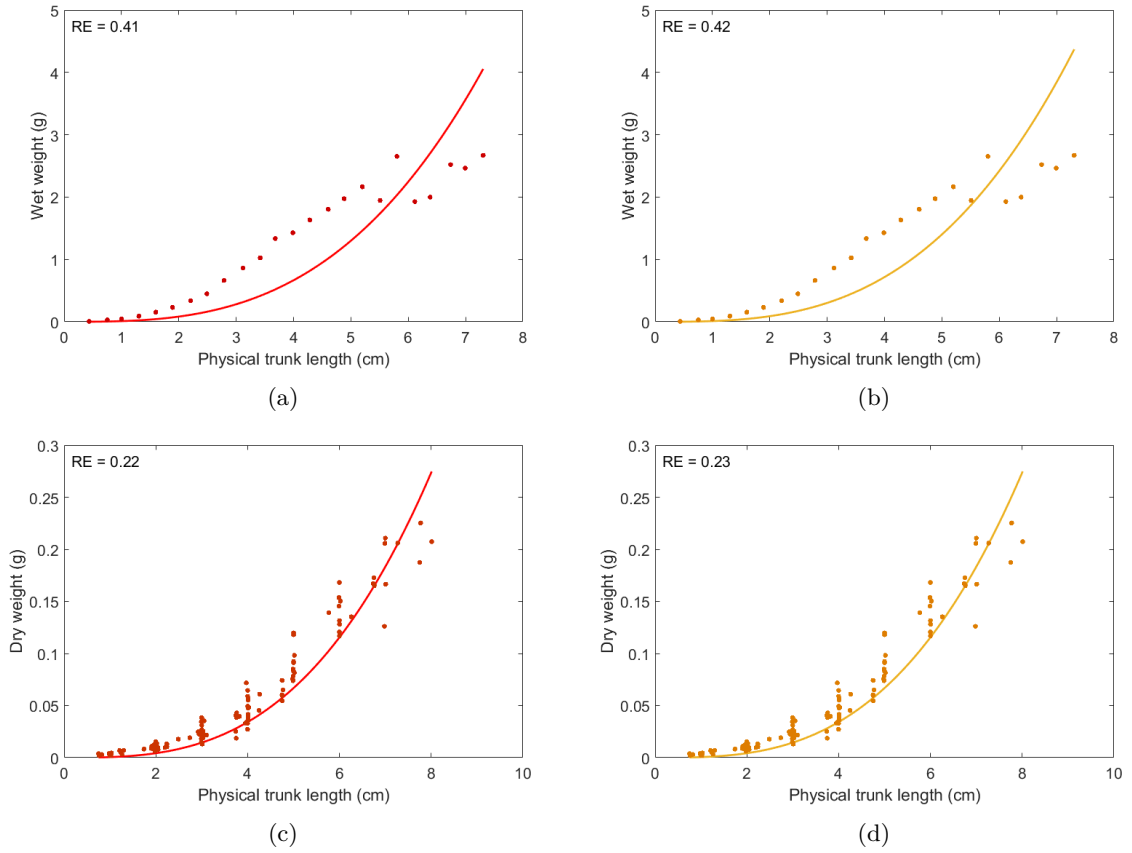
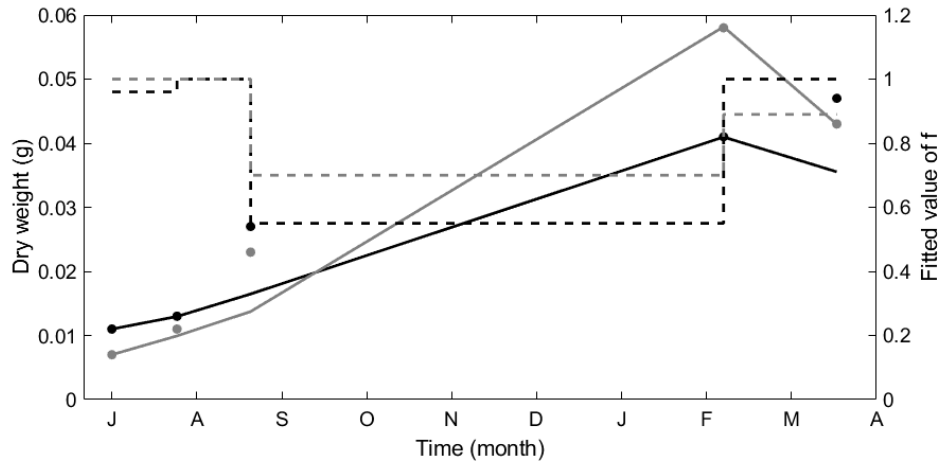
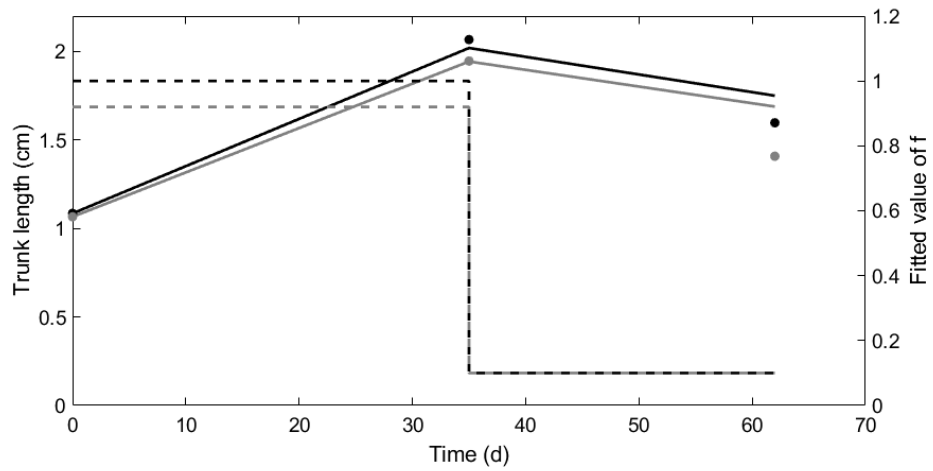


Figure 7: Data (dots) and predictions (lines) of the wet weight as a function of trunk (a,b) and total (b,c) length for *Arenicola marina* individuals collected at Wimereux (this study) and of the dry weight as a function of trunk length (e,f) for *A. marina* (data from De Wilde and Berghuis (1979)) using both an abj-DEB model (a,c,e) and a std-DEB model (b,d,f). The corresponding values of the shape coefficient are: (a) $\delta_M = 0.20$ (b) $\delta_M = 0.13$ (c) $\delta_M = 0.14$ (d) $\delta_M = 0.09$. RE stands for relative error.

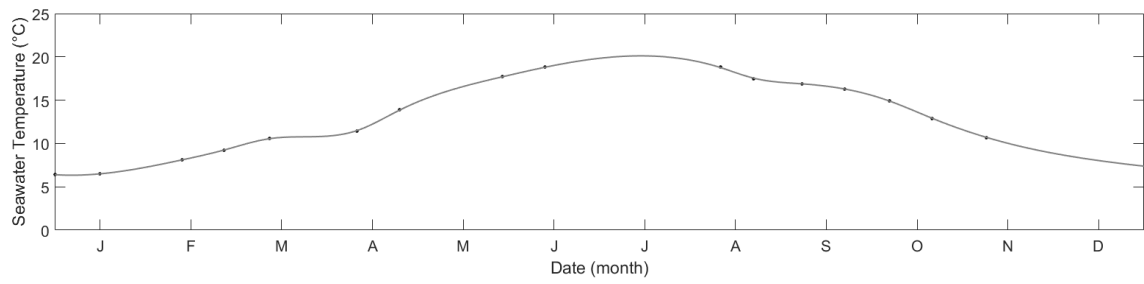


(a)

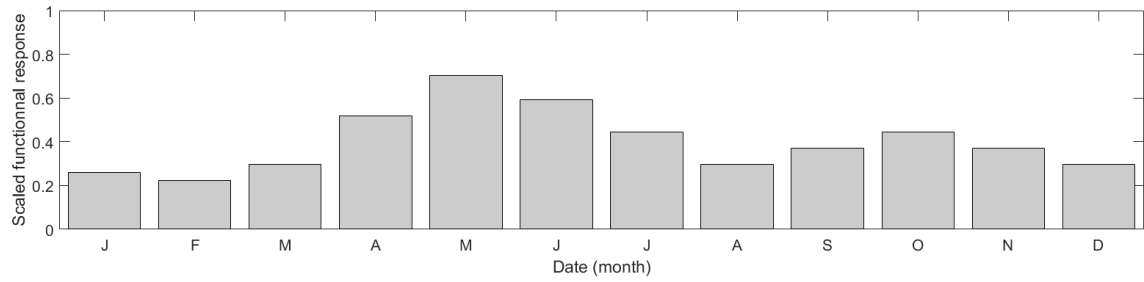


(b)

Figure 8: Reconstruction of the scaled functional response value (f , dashed lines) from field (a) and experimental (b) data (dots) with the abj-model for *Arenicola marina* from this study (lines are the model predictions). The observations of a field growth survey of *A. marina* (dots) are taken from Beukema and De Vlas (1979) in two beaches of the Wadden Sea (black and grey). The associated predictions of the DEB model (lines) for the best fitted values of f (dashed lines) are represented. Sea surface temperature were taken from Van Aken (2008). The laboratory observations (dots) on growth in trunk length of *Arenicola marina* in different feeding conditions (fed in black and unfed in grey) are associated to the growth predictions of the DEB model (lines) with the fitted values of the scaled functional response f (dashed lines) for $T = 16.5^{\circ}\text{C}$.



(a)



(b)

Figure 9: *In situ* temperature of the seawater at Wimereux (Hauts-de-France, Eastern English Channel) during the year 2017 (a), and estimated scaled functional response f at this site (b), used for the predictions of the chronology of the first life stages of the life cycle of *Arenicola marina* and of the wet weight and trunk length growth of the species at this site.

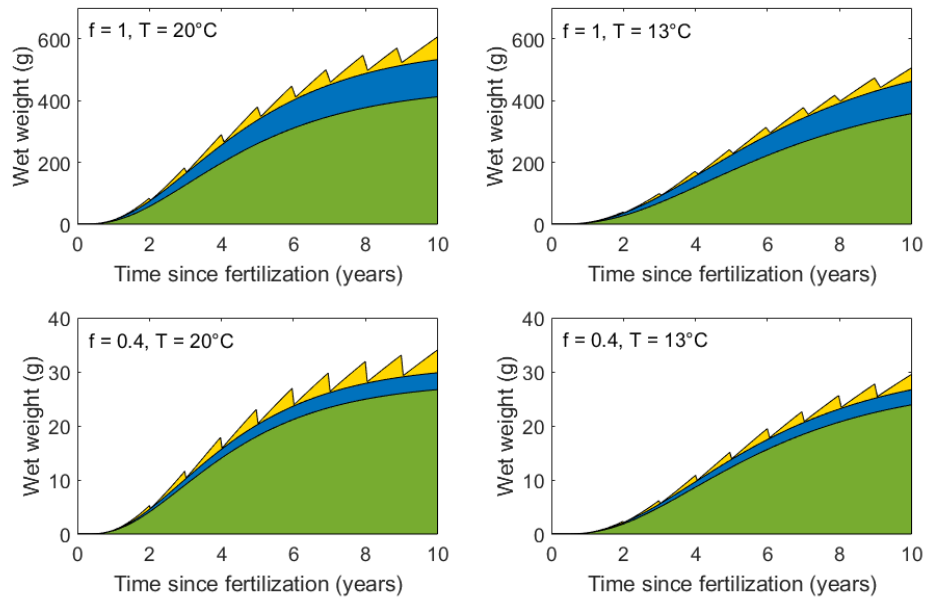


Figure 10: Predictions of the abj-DEB model of the evolution of the wet weight of the structure S (green), the reserve E (blue) and the reproduction buffer E_R (yellow) compartments of *Arenicola marina* under different environmental conditions from fertilization time: $f = 1$ (food available *ad libitum*) & $T = 20^\circ\text{C}$; $f = 1$ & $T = 13^\circ\text{C}$; $f = 0.4$ & $T = 20^\circ\text{C}$; $f = 0.4$ & $T = 13^\circ\text{C}$ (mean environmental conditions found at Wimereux).

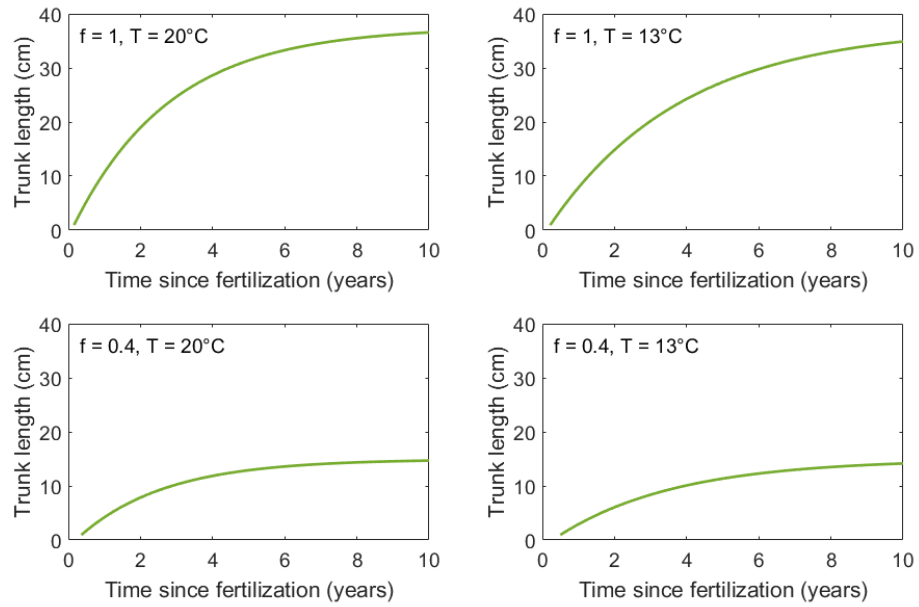


Figure 11: Predictions of the abj-DEB model of the evolution of the trunk length of *Arenicola marina* under different environmental conditions ($f = 1$ & $T = 20^\circ\text{C}$; $f = 1$ & $T = 13^\circ\text{C}$; $f = 0.4$ & $T = 20^\circ\text{C}$; $f = 0.4$ & $T = 13^\circ\text{C}$) from the age at puberty a_p .

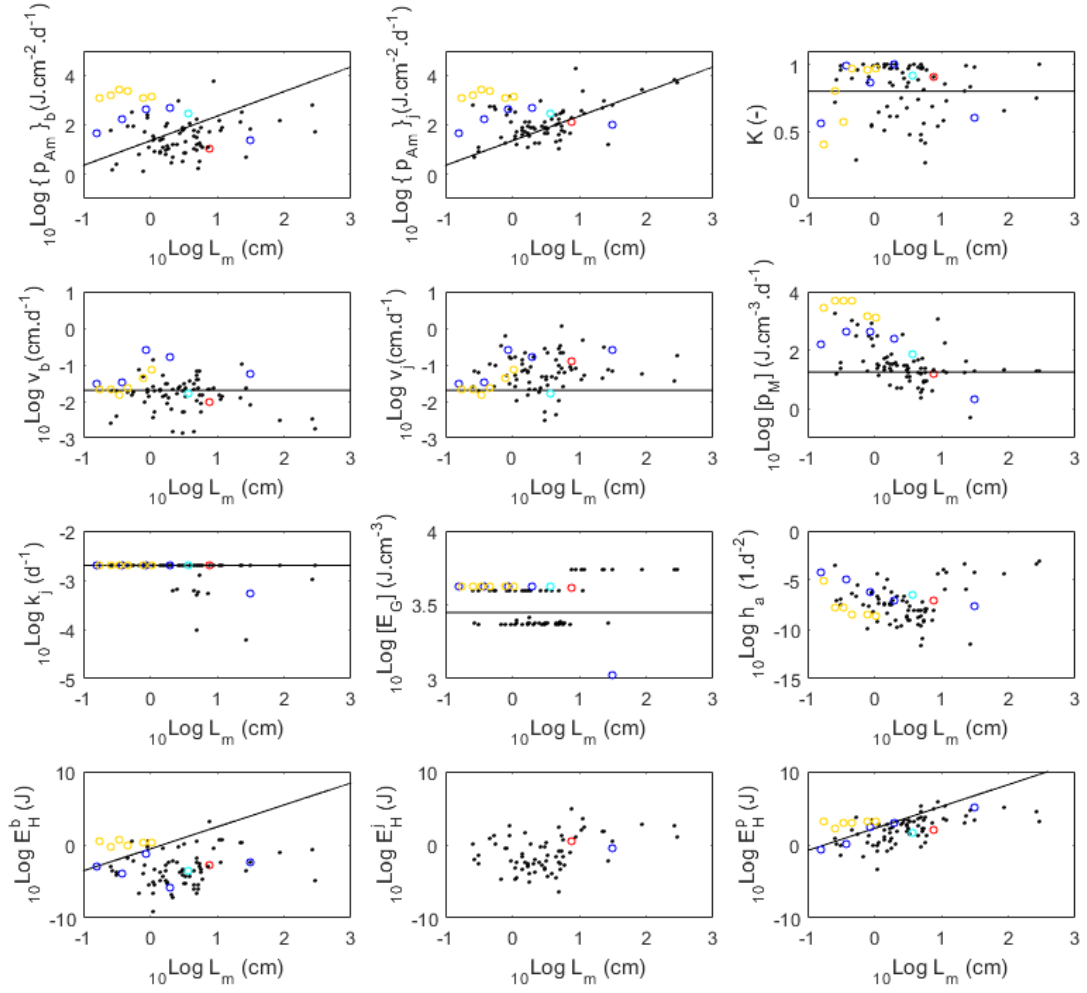


Figure 12: Comparison of log-log plots of $\{\dot{p}_{Am}\}_b$ at birth and $\{\dot{p}_{Am}\}_j$ after the metamorphosis, κ , \dot{v}_b at birth and \dot{v}_j after the metamorphosis, $[p_M]$, k_j , $[E_G]$, h_a , E_H^b , E_H^j , and E_H^p in Mollusca (black), Annelida Clitellata (yellow), Annelida Polychaeta (blue), standard model values for *Arenicola marina* (cyan) and abj model values from this study (red). $\{\dot{p}_{Am}\}$ is the maximum assimilation rate, κ the fraction of mobilised reserve allocated to soma, \dot{v} the energy conductance, $[p_M]$ the specific somatic maintenance costs, k_j the maturity maintenance rate coefficient, $[E_G]$ the costs of structure, h_a the Weibull ageing acceleration, and E_H^b , E_H^j , and E_H^p the maturity thresholds for birth, metamorphosis and puberty. The lines correspond to expectations on the basis of the generalized animal (Kooijman, 2010, Table 8.1).

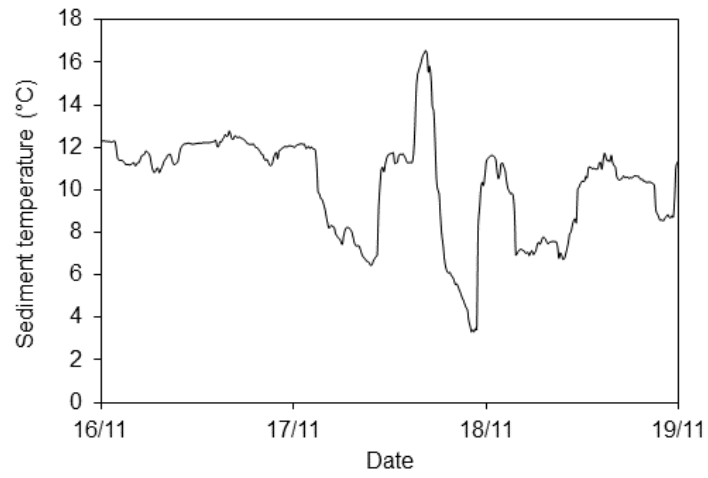


Figure 13: Sediment temperature (upper shore, 10 cm deep) recorded every 10 min at Wimereux (Hauts-de-France, Eastern English Channel) between the 16 of November and the 19 of November 2017 with a HOBO probe.

Table 1: State variables, fluxes, metric relationships, acceleration and shape coefficient of the abj-DEB model and associated mathematical expressions (Kooijman, 2014; Kooijman and Lika, 2014; Kooijman, 2010; Van der Meer, 2006). L is the structural length (cm) with $L = V^{1/3}$, and L_b and L_j are the structural lengths at birth and metamorphosis respectively. d_V is the density of wet structure, d_E the density of wet reserve, d_{Ed} the density of dry reserve, μ_{Ed} the specific chemical potential of reserve and w_{Ed} the molar weight of dry reserve. $L_w(t)$ is the physical total length at time t of the organism and $TL_w(t)$ its physical trunk length. $W_w(t)$ is the wet weight at time t of the organism. If $E_H^j = E_H^b$ the abj- model reduces to the std- model.

State variables	Reserve	$\frac{dE}{dt} = \dot{p}_A - \dot{p}_C$
	Structure	$\frac{dV}{dt} = \frac{\dot{p}_G}{[E_G]}$
	Maturity	if $E_H < E_H^p$ $\frac{dE_H}{dt} = \dot{p}_H$; else $\frac{dE_H}{dt} = 0$
	Allocation to reproduction	if $E_H \geq E_H^p$, $\frac{dE_R}{dt} = \kappa_R \cdot \dot{p}_R$; else $\frac{dE_R}{dt} = 0$
Fluxes	Ingestion	$\dot{p}_X = \frac{\dot{p}_A}{\kappa_X}$
	Assimilation	$\dot{p}_A = \{\dot{p}_{Am}\} \cdot s_M \cdot f \cdot V^{2/3}$
	Mobilisation	$\dot{p}_C = E \cdot \frac{\dot{v} \cdot s_M \cdot V^{2/3} \cdot [E_G] + \dot{p}_S}{\kappa \cdot E + V \cdot [E_G]}$
	Somatic maintenance costs	$\dot{p}_S = [\dot{p}_M] \cdot V$
	Maturity maintenance costs	$\dot{p}_J = \dot{k}_J \cdot E_H$
	Growth	$\dot{p}_G = \kappa \cdot \dot{p}_C - \dot{p}_S$
	Reproduction	$\dot{p}_R = (1 - \kappa) \cdot \dot{p}_C - \dot{p}_J$
	Maturity	$\dot{p}_H = (1 - \kappa) \cdot \dot{p}_C - \dot{p}_J$
Metric relationships	Physical length (cm)	$L_w(t) = \frac{V(t)^{1/3}}{\delta}$
	Wet weight (g)	$W_w(t) = d_V \cdot V(t) + (E(t) + E_R(t)) \cdot \frac{w_{Ed} \cdot d_E}{\mu_{Ed} \cdot d_{Ed}}$
Acceleration coefficient	if $E_H < E_H^b$ $s_M = 1$; if $E_H^b \leq E_H < E_H^j$ $s_M = L/L_b$; else $s_M = L_j/L_b$ if $E_H \geq E_H^j$	
Shape coefficient	if $E_H < E_H^b$ $\delta = \delta_{Me}$; if $E_H^b \leq E_H < E_H^j$ $\delta = \delta_{Me} + (\delta_M - \delta_{Me}) \cdot (\frac{L - L_b}{L_j - L_b})$; else $\delta = \delta_M$ if $E_H \geq E_H^j$	

Table 2: Abiotic and biometric data related to the samples of *Arenicola marina* collected at Wimereux, Le Touquet and Fort Mahon and used later on for the parameter estimation of a DEB-model for *A. marina*

Type of data	Number of samples	Collection date	Temperature (°C)	Wet weight (g)		Trunk length (cm)	
				range	mean	range	mean
Oxygen consumption	39	16/05/2018	12	0.00 - 3.73	1.10 ± 1.00	0.36 - 5.60	2.85 ± 1.52
	63	13/06/2018	15	0.02 - 5.70	1.39 ± 1.69	0.80 - 7.30	2.95 ± 1.82
	55	25/07/2018	20.5	0.03 - 5.91	0.92 ± 1.33	0.90 - 6.80	2.64 ± 1.50
Growth	290	26/05/2018	13	0.00 - 0.11	0.05 ± 0.02	0.40 - 1.60	1.10 ± 0.20
Reproduction	9	Sept. to Nov. 2016 to 2018	13	2.30 - 17.60	6.10 ± 5.60	4.20 - 13.00	7.40 ± 3.70

Table 3: Data used in the abj- and std- model parameters estimations for *Arenicola marina* among the available dataset. The age and length at metamorphosis were only used for the abj-model parameter estimation.

Type of data	Data	References
Zero-variate	age at trochophore larva	Pers. comm. from S. Gaudron
	age at birth	Farke and Berghuis (1979)
	age at metamorphosis	Farke and Berghuis (1979)
	age at puberty	De Cubber et al. (2018)
	lifespan	Beukema and De Vlas (1979), De Cubber et al. (2018)
	egg diameter	Watson et al (1998), De Cubber et al. (2018)
	total length of the trochophore larva	Farke and Berghuis (1979)
	total length at birth	Farke and Berghuis (1979)
	total length at metamorphosis	Farke and Berghuis (1979)
	trunk length at puberty	De Cubber et al. (2018)
	total maximum length	Pers. comm. from S. Gaudron (Sorbonne Univ.)
	wet weight of an egg	This study
Uni-variate	TL-Ww	This study
	TL-Wd	De Wilde and Berghuis (1979)
	t-TL (4 temperatures, 2 feeding conditions)	De Wilde and Berghuis (1979)
	t-Ww (2 feeding conditions)	Olive et al.(2006)
	Ww-O2 (3 temperatures, experimental conditions)	This study
	TL-R	This study

Table 4: Summary of the primary and some auxiliary parameters provided by the parameter estimation of the std- and the abj-DEB models for *Arenicola marina*

Parameter	Symbol	Value		Unit
		std-model	abj-model	
Reference temperature ¹	T_{ref}	293.15	293.15	K
Fraction of food energy fixed in reserve ¹	κ_X	0.80	0.80	-
Arrhenius temperature	T_A	3800	3800	K
Energy conductance ²	\dot{v} (\dot{v}_j)	1.67 e ⁻⁰² (-)	9.79 e ⁻⁰³ (0.12)	cm.d ⁻¹
Allocation fraction to soma	κ	0.92	0.92	-
Reproduction fraction fixed in eggs ¹	κ_R	0.95	0.95	-
Volume specific costs of structure	$[E_G]$	4173	4127	J.cm ⁻³
Maturation threshold for the trochophore larva	E_H^{tr}	2.73 e ⁻⁰⁴	8.44 e ⁻⁰⁴	J
Maturation threshold for birth	E_H^b	2.73 e ⁻⁰⁴	1.27 e ⁻⁰³	J
Maturation threshold for metamorphosis	E_H^j	-	1.94	J
Maturation threshold for puberty	E_H^p	38.62	104.50	J
Weibull ageing acceleration	\ddot{h}_a	3.08 e ⁻⁰⁷	6.69 e ⁻⁰⁸	d ⁻²
Gompertz stress coefficient ¹	s_G	1.00 e ⁻⁰⁴	1.00 e ⁻⁰⁴	-
Acceleration rate ³	s_M	-	11.46	-
Maximum assimilation rate ²	$\{\dot{p}_{Am}\}$ ($\{\dot{p}_{Am}\}_j$)	280.08 (-)	10.62 (130.63)	J.cm ⁻² .d ⁻¹
Specific somatic maintenance rate	$[\dot{p}_M]$	69.89	15.82	J.cm ⁻³ .d ⁻¹
Maturity maintenance rate ¹	\dot{k}_J	2.00 e ⁻⁰³	2.00 e ⁻⁰³	d ⁻¹
Specific density of wet structure ¹	d_V	1	1	g.cm ⁻³
Specific density of wet reserve ¹	d_E	1	1	g.cm ⁻³
Specific density of dry reserve ¹	d_{Ed}	0.16	0.16	g.cm ⁻³
Specific chemical potential of dry reserve ¹	μ_{Ed}	550000	550000	J.Cmol ⁻¹
Molar weight of dry reserve ¹	w_{Ed}	23.9	23.9	g.Cmol ⁻¹

¹ Fixed parameters. The values were taken from the generalized animal (Kooijman, 2010).

² The values inside brackets are the ones after metamorphosis when using the abj-model: $\dot{v}_j = s_M \cdot \dot{v}$ and $\{\dot{p}_{Am}\}_j = s_M \cdot \{\dot{p}_{Am}\}$

³ s_M is given for a scaled functional response of 1 after metamorphosis

Table 5: Summary of the zero-variate observations values and associated predictions and relative errors (RE) obtained with both the abj- and the std-DEB models for *Arenicola marina*

Data	Symbol	Value	Predictions (RE)		Unit
			std-model	abj-model	
age at trochophore larva	a_{tr}	7	2.769 (0.60)	7.7 (0.1)	d
age at birth	a_b	30	2.774 (0.91)	10.52 (0.65)	d
age at metamorphosis	a_j	78	-	89.68 (0.15)	d
age at puberty	a_p	548	142.9 (0.74)	174.5 (0.68)	d
lifespan	a_m	2190	2194 (0.02)	2462 (0.12)	d
egg diameter	L_0	0.02	0.020 (0.02)	0.021 (0.07)	cm
total length of the trochophore larva	L_{tr}	0.025	0.014 (0.45)	0.019 (0.20)	cm
total length at birth	L_b	0.08	0.014 (0.83)	0.023 (0.71)	cm
total length at metamorphosis	L_j	0.89	-	0.85 (0.05)	cm
trunk length at puberty	TL_p	2.5	3.2 (0.28)	3.17 (0.27)	cm
maximum trunk length	TL_i	34	27.58 (0.19)	37.4 (0.10)	cm
wet weight of an egg	Ww_0	4.78 e^{-6}	4.45 e^{-6} (0.07)	5.15 e^{-6} (0.08)	g

Table 6: Predictions on the chronology and lengths of different life cycle stages of *Arenicola marina* according to the *in situ* environmental conditions at Wimereux (Hauts-de-France, Eastern English Channel) made by the abj-DEB model.

Event	Length (cm)	Age (d)
Trochophore larva	0.021	10.29
Birth (first feeding)	0.034	15.51
End of the metamorphosis	1.12	208.26
Puberty	3.50	373.19